

Multi-period Design and Planning Model of Shale Gas Field Development

Zedong Peng¹ | Can Li² | Ignacio E. Grossmann² |
Kysang Kwon³ | Sukjoon Ko³ | Joohyun Shin³ |
Yiping Feng¹

¹Department of Control Science and Technology, Zhejiang University, Hangzhou, Zhejiang, 310027, China

²Department of Chemical Engineering, Carnegie Mellon University, Pittsburgh, PA, 15213, USA

³Optimization and Analytics Lab, SK Innovation, Seoul, 110-728, South Korea

Correspondence

Ignacio E. Grossmann, Department of Chemical Engineering, Carnegie Mellon University, Pittsburgh, PA 15213, USA
Email: grossmann@cmu.edu

Funding information

China Scholarship Council; SK Innovation

Long-term design and planning of shale gas field development is challenging due to the complex development operations and a wide range of candidate locations. In this work, we focus on the multi-period shale gas field development problem, where the shale gas field has multiple formations and each well can be developed from one of several alternative pads. The decisions in this problem involve the design of the shale gas network and the planning of development operations. A mixed-integer linear programming (MILP) model is proposed to address this problem. Since the proposed model is a large-scale MILP, we propose a solution pool based bilevel decomposition algorithm to solve it. Results on realistic instances demonstrate the value of the proposed model and the effectiveness of the proposed algorithm.

KEYWORDS

Shale gas field development, production shut-in, mixed-integer linear programming, bilevel decomposition

Introduction

According to the Annual Energy Outlook 2020 by U.S. Energy Information Administration [1], dry natural gas has taken the leading position in the U.S. energy production market. Dry natural gas production has an average annual

growth rate of 5.1% from 2015 to 2020 in Figure 1. The main drive behind the growth is the boom of the shale gas revolution. Dry natural gas produced by tight/shale gas accounts for 83.9% of the total production in the U.S., and this rate is expected to grow to 91.3% in 2050. Due to the domestic production growth, the imports of natural gas continue to decline from historical levels, and the liquefied natural gas (LNG) exports will continue to rise through 2030. The shale gas revolution, in a sense, has changed the U.S. energy market.

The first commercial shale gas well was first drilled in Fredonia, New York, in 1821. However, it is the recent technology developments that has given access to large volumes of shale gas, which were previously uneconomical to produce. The key technologies include horizontal drilling, hydraulic fracturing, multi-well pads and walking rig. Horizontal drilling and hydraulic fracturing are now standard practice for shale gas development. Shale ordinarily has insufficient matrix permeability to allow significant fluid flow to a wellbore and the shale gas is trapped in the shale formation. Horizontal drilling enables the well to penetrate a greater section of the reservoir and increase the contact between the borehole and the shale formation. Next, a pressurized liquid is pumped into a wellbore to create cracks in the shale formation to increase its permeability. This process is called hydraulic fracturing, which provides the trapped oil and natural gas a conductive flow path into the wellbore. The horizontal drilling technology gives rise to multi-well pad drilling, another one of the most influential innovations in shale gas development. The multi-well pad is a location that houses the wellheads for several horizontal wells drilled in different directions. This technology enables the producers to drill 2 to 40 horizontal wells from a single pad. It allows rig operators to drill groups of wells more efficiently than one well per site since it saves the time to move from one well location to the next. Walking rig technology is also leading to efficiency gains for oil and gas producers. Compared with the previous high cost of disassembling and reassembling rigs, it is more efficient to build a road between two pads and transport the entirely constructed rigs using walking or skidding systems.

Generally, the development of a shale gas field takes a long term for up to several years. The gathering system is usually constructed in the first place to transport the oil, gas and saltwater produced from each well. Once the gathering system is completed, multiple wells are developed in the field. The development of each well begins with constructing the pad, where a rig is set up to drill horizontal wells and surface facilities for production are installed. After all these preparations, the well is first vertically drilled down to the selected shale gas formation and then horizontally drilled to increase the exposed section length through the reservoir. Next, it proceeds to completion operations. The well will be hydraulic fractured to extract the oil and gas from the formation. Once the development completed, the well is turned in line to produce gas and oil.

In shale gas development, there is a tradeoff in the development speed due to the production decline of shale gas wells [2]. When shale gas wells are turned in line to produce oil and gas, the production begins with a medium level and then goes up rapidly to the peak. After that, the production declines continuously. The decline in the first two or three years is drastic. After this period, the production levels off for the next 10 or 15 years. Therefore, if the development is performed intensively and most of the wells are turned in line at the same time, it requires a huge gathering system during the early period of the development. However, two or three years later, the production declines and the overcapacity will show up in the gathering system. Return-to-pad is a strategy to alleviate the poor use of gathering system in later periods. When the production of the developed well declines, new wells can be developed on the same pad. Therefore, the total production of the pad will increase again.

In this paper, a mixed-integer linear programming model is proposed to find the most profitable development strategy and pipeline installation strategy. The paper is organized as follows. In section 2, the review of related literature in the field of shale gas development is presented. In section 3, the detailed statement, the main assumptions and the superstructure of this problem are given. In section 4, the problem is formulated as a mixed-integer linear programming model. To efficiently solve the model, a bilevel decomposition algorithm is proposed in section 5. Five

examples are tested to demonstrate the efficiency of the proposed algorithm in section 6. The optimal development decisions of two examples are further analyzed to demonstrate the value of the proposed model. Finally, the paper ends up with the conclusion drawn from the results of the case studies.

Related work

Compared with the long-term studies on conventional oil and gas field development, it is recently that optimization technologies are applied to improve efficiency the shale gas development. Several topics have received attention, including planning and design, water management, refracturing and shut-in management.

The planning and design of shale gas field development range in scales from the detailed scheduling of development operations to strategic planning. Cafaro and Grossmann [3] first proposed a mixed-integer nonlinear programming (MINLP) model for the long-term planning of the shale gas supply chain in 2014. The decisions include the number of wells to drill at every location, the size of gas processing plants, the section and length of pipelines for gathering raw gas and delivering processed gas and by-products, the power of gas compressors, and the amount of freshwater required from reservoirs for drilling and hydraulic fracturing to maximize the net present value of the project. Based on this work, Drouven and Grossmann [4] extend the shale gas development problem by considering strategic decisions, such as the arrangement of delivery agreements and the selection of the preferred downstream delivery nodes. Besides the extension of decisions, the discrete size of pipelines and compressors is also introduced. Focusing more on the scheduling of development operations, Ondeck and Drouven [5] addressed the single multi-well pad development problem by proposing a MILP model. The environmental impact of shale gas development is being researched recently. Gao and You [6, 7, 8] published several works that integrate economic benefit and life-cycle environments impact together as the optimization objective.

Water management is another critical topic in shale gas development since hydraulic fracturing requires a tremendous amount of water [9]. Yang et al. [10] proposed an investment optimization model based on the State-Task Network framework to determine the location and capacity of impoundment, the type of piping, treatment facility locations and removal capability, freshwater sources and fracturing schedule. Drouven and Grossmann [11] presented a mixed-integer linear programming model to support upstream operators in identifying optimal strategies for impaired water management in active shale gas development areas. Instead of optimizing water management strategy alone, Guerra et al. [12] presents an integrated framework for water management and shale gas supply chain design.

There are also some publications dealing with the special operations in shale gas development, like refracturing and shut-in. Cafaro and Drouven [13] proposed a discrete-time MILP model to find the optimal refracture treatment strategy to increase each well's profitability. Following this work, they [14] also proposed a novel continuous-time multi-refracture planning model to address the same problem. Since the refracturing performance differs among wells, Asala and Chebeir [15] proposed an integrated machine learning and optimization method to determine the best refracturing strategy. Besides refracturing, shut-ins can also lead to pressure build-up in the wellbore and the nearwell region of the reservoir. Knudsen and Foss [16] proposed a cyclic shut-in and production strategy to avoid the well liquid loading by solving a generalized disjunctive program (GDP). Similar to shut-ins, artificial lift methods(ALM) are also used to lift the accumulated fluids in the well and to help sustain well performance. Zeng and Cremaschi [17] proposed both a deterministic MILP model and a stochastic model under uncertain ALM-dependent production rates for artificial lift infrastructure planning. Focusing on the pooling system, Li et al. [18] proposed a stochastic pooling problem optimization formulation for natural gas production network design and operation.

In this paper, an MILP model is proposed to determine the most profitable shale gas field development strategy. The main contributions of this work include:

1. A novel superstructure is proposed for the shale gas field development problem motivated by a real-world case. In this superstructure, a more realistic correlation between wells and pads is considered compared with previous works like [3]. A candidate well can be developed from several alternative candidate pads. Therefore, instead of determining the number of wells to be developed in each pad, we need to determine the detailed development operations scheduling of a candidate well and the connection between wells and pads.

2. It is often the case that there is more than one formation in the shale gas field. The proposed MILP model is capable of multi-formation shale gas field development.

3. Shut-in is also included in the proposed model. Instead of using shut-in as a pressure build-up technology, we consider shut-in as a measure to guarantee the development process's safety during hydraulic fracturing.

4. A bilevel decomposition algorithm is proposed to solve the proposed MILP model more efficiently. The solution pool is applied to enhance the performance of the bilevel decomposition algorithm.

Problem statement

The shale gas field development problem can be stated as follows. The given untapped shale gas field has more than one formation and is divided into several sections. A set of candidate wells, pads, gas injection points and pipeline locations have been determined in advance. In each section, there are five candidate pad locations and five candidate well locations. The pads and junctions are placed along the borders of sections. Both formations in this field can be developed and the production profile of the two formations are different. The candidate wells in the same formation and same section have the same production profile. The production profile forecast of each section across periods is given. The pipelines are only used to transport gas. Oil is separately transported by trunks, which is out of scope in this problem. We need to determine the most profitable development strategy and pipeline installation strategy.

Based on the statement above, we summarize the superstructure of the shale gas field. An example of the shale gas field superstructure with two formations is given in Figure 2. In the superstructure, each well w can be developed from a set of pads $p \in P(w)$. In turn, the wells that can be developed from pad p are defined as set $W(p)$. Each pad p can be connected by candidate pipelines to adjacent pads $p' \in P(p)$ or gas junction points $j \in J$. There is one delivery point in the shale gas field. Wells are divided into two categories, 2D well and 3D well, according to the well-pad connection as shown in Figure 2. 2D well means the pad and well are located in the same location, while 3D wells mean the horizontal coordinates of the well and the connected pad differ. It takes more effort to develop a 3D well than a 2D well since inclined vertical drilling is required when developing a 3D well. According to assumptions 1 and 3, there are four operations for each well, including drilling, completion, production and shut-in.

The decisions of this shale gas development problem include well development decisions and pipeline installation decisions. The well development decisions involve: a) when and which candidate wells to be drilled in each section, b) which pad should the wells be connected to, c) whether the developed wells need to be shut-in, d) when and where to allocate rigs across over time. The pipeline installation decisions involve: a) when and where to layout pipelines, b) which size of pipelines to be installed.

Assumptions

The major assumptions for this problem are as follows:

1. As mentioned above, the operations to develop a shale gas well include pad construction, rig relocation, vertical drilling, horizontal drilling, hydraulic fracturing and turning in line. To simplify the development operations, we aggregate the whole process into two primary operations, drilling and completion. Multiple pads can be set up at the

same period. However, at most one well can be developed in each pad at each time period.

2. The planning horizon is discretized into a set of time periods with equal lengths. Depending on the different choice of the length of each period, some operations may take several time periods to finish. It is assumed that operations cannot be stopped half-way once they have started.

3. After completion, wells start to produce gas and oil unless shut-in happens.

4. According to the distance between each pad and delivery point, flow directions within the proposed pipeline superstructure are determined in advance. For example, the flow direction of the superstructure in Figure 2 is determined as labelled.

5. There is a limit of scope that hydraulic fracture can only cover vertically in the formation. When the formation is thick, several wells may be horizontally drilled in different depths at the same location to fully extract the trapped shale gas in the formation. However, in this work, we assume that only one well can be developed in each formation at the same location.

6. Generally, temporary shut-in of working wells will lead to an increase in the pressure of the well. To simplify the change of the production profile, we assume that there is simply a production delay if shut-in happens. But the absolute production rates are not affected by shut-in afterwards. We also assume that each well is independent and we do not consider the interference between wells.

7. The composition of shale gas produced in each candidate well is assumed the same and known in advance.

8. The gas pressure drop in pipelines is assumed to be zero. Therefore, the installation of compressors is not considered in this problem.

9. Since the pipelines are usually standardized in the oil and gas industry, it is assumed that the alternative pipeline diameters are discrete.

10. To handle the nonlinear nature of production decline curve of shale gas, the production profile of each well is discretized to a given value for each period.

11. The price of the oil and natural gas are assumed to be constant throughout the whole planning horizon.

12. It is assumed that there is only one delivery node in the shale gas field.

13. Water management is not considered in this problem.

Mathematical formulation

In this section, the multi-period multi-formation shale gas field development problem is formulated as a discrete-time mixed-integer linear programming (MILP) model.

| Well development constraints

To represent the assignment of development operations and the connections between wells $w \in W$ and pads $p \in P$ at both formations $f \in F$, we introduce binary variables $y_{w,p,f,t}^{DRILL}$ for drilling operation and $y_{w,p,f,t}^{COMP}$ for completion operation. Since it may take several periods to finish one operation, the duration of the drilling operation is defined by the parameter τ_D . For the whole planning horizon, each well corresponding to each formation $f \in F$ can only be developed once. According to assumption 5, both formations can be developed at the same well location. We formulate this constraint as Eq.(1).

$$\sum_{p \in P(w)} \sum_{t \in T} y_{w,p,f,t}^{DRILL} \leq 1 \quad \forall w \in W, f \in F \quad (1)$$

The number of wells that can be drilled at each pad in each period is generally constrained by the pad's size and the number of crews and equipment assigned to each pad. According to assumption 1, at most one drilling operation can be implemented at each pad at each time t .

$$\sum_{w \in W(p)} \sum_{f \in F} \sum_{t - \tau_D + 1 \leq \tau \leq t} y_{w,p,f,\tau}^{DRILL} \leq 1 \quad \forall p \in P, t \in T \quad (2)$$

For the development of each well, the completion operation is not allowed to start until the drilling operation is finished. There are two formulations to express the sequence logic in scheduling problems, time-aggregated formulation and time-disaggregated formulation. The time-aggregated formulation is Eq.(3) and the time-disaggregated formulation is as Eq.(4) [5, 19]. The computational performance of these two formulations is evaluated in our case studies.

$$\sum_{t \in T} t \cdot y_{w,p,f,t}^{COMP} \leq \sum_{t \in T} (t + \tau_D) \cdot y_{w,p,f,t}^{DRILL} \quad \forall w \in W, p \in P(w), f \in F \quad (3)$$

$$y_{w,p,f,t}^{COMP} \leq \sum_{\tau \leq t - \tau_D} y_{w,p,f,\tau}^{DRILL} \quad \forall w \in W, p \in P(w), f \in F, t \in T \quad (4)$$

In the shale gas industry, the pad-drilling batch is a series of drilling operations where multiple wells are sequentially developed from a pad. All wells developed in a pad drilling batch should be online at the same because of safety reasons. Small batch size means that the wells can start production at relatively early time periods. Therefore, the revenue from these wells also arrive early but at the expense of higher operation costs such as rig set-up cost. In a drilling batch, completion can not start until the drilling operations of all wells in this pad-drilling batch have finished.

$$y_{w,p,f,t}^{COMP} \leq 1 - \sum_{w' \in W(p)} \sum_{f' \in F} \sum_{t - \tau_D + 1 \leq \tau \leq t} y_{w',p,f',\tau}^{DRILL} \quad \forall w \in W, f \in F, p \in P, t \in T \quad (5)$$

Compared with drilling, the duration of completion operation for each well is much shorter. Here, we defined a parameter n_1^C in Eq.(6) as an upper limit number of wells that can be hydraulically fractured from each pad in each time period.

$$\sum_{w \in W(p)} \sum_{f \in F} y_{w,p,f,t}^{COMP} \leq n_1^C \quad \forall p \in P, t \in T \quad (6)$$

Since hydraulic fracturing requires a large amount of water and the available water supply in the shale gas field is

limited, there is an upper limit for the number of wells that could be hydraulically fractured in each time period.

$$\sum_{w \in W} \sum_{p \in P(w)} \sum_{f \in F} y_{w,p,f,t}^{COMP} \leq n_2^c \quad \forall t \in T \quad (7)$$

All operations on well w have to be finished in the planning horizon if the drilling operation starts, i.e., no well can be left unfinished within the planning horizon.

$$\sum_{t \in T} y_{w,p,f,t}^{DRILL} = \sum_{t \in T} y_{w,p,f,t}^{COMP} \quad \forall w \in W, f \in F, p \in P \quad (8)$$

Shut-in related constraints

In the development of a shale gas well, many risks need to be considered. Hydraulic fracturing is one of them since it involves the high-pressure injection of fracking fluid into a wellbore to create cracks. For safety reasons, two situations will result in the working well w shut-in and three conditions are related to this.

- Condition 1. The nearby wells w' of well w at the same formation are being completed
- Condition 2. Return-to-pad happens to the same pad where well w is developed and the new well w' is being completed.
- Condition 3. Well w is developed and is producing gas and oil.

Only when condition 1 and condition 3 or condition 2 and condition 3 simultaneously hold, the production of well w will shut in. We use Generalized Disjunctive Programming(GDP) [20] to model this logic constraint. Three Boolean variables are introduced. $Y_{w,p,f,t}^1$ represents if the development of well w at formation f connected to pad p is finished at time t . $Y_{w,p,f,t}^2$ represents if well w at formation f connected to pad p is being completed at time t . $Y_{w,p,f,t}^{SHUTIN}$ represents if well w at formation f connected to pad p should be shut-in at time t . The logic constraint can be formulated as Eq.(9).

$$\left[Y_{w,p,f,t}^1 \wedge \left(\bigvee_{w' \in W(w), \forall p' \in P(w')} Y_{w',p',f,t}^2 \right) \right] \vee \left[Y_{w,p,f,t}^1 \wedge \left(\bigvee_{w' \in W(p), f' \in F} Y_{w',p',f',t}^2 \right) \right] \Leftrightarrow Y_{w,p,f,t}^{SHUTIN} \quad \forall w \in W, p \in P(w), f \in F, t \in T \quad (9)$$

where $W(w)$ is the set of wells near well w . Based on the logic constraint, we can transform Eq.(9) into the Conjunctive Normal Form (CNF) as Eq.(10-11).

$$w' \in W(w), \forall p' \in P(w') \left[\neg Y_{w,p,f,t}^1 \vee \neg Y_{w',p',f,t}^2 \vee Y_{w,p,f,t}^{SHUTIN} \right] \wedge \left[\bigwedge_{w' \in W(p), f' \in F} \left[\neg Y_{w,p,f,t}^1 \vee \neg Y_{w',p',f',t}^2 \vee Y_{w,p,f,t}^{SHUTIN} \right] \right] \quad \forall w \in W, p \in P(w), \quad (10)$$

$$\left[-Y_{w,p,f,t}^{SHUTIN} \vee Y_{w,p,f,t}^1 \right] \wedge \left[-Y_{w,p,f,t}^{SHUTIN} \vee \left(\bigvee_{w' \in W(w), \forall p' \in P(w')} Y_{w',p',f,t}^2 \right) \vee \left(\bigvee_{w' \in W(p), f' \in F} Y_{w',p',f',t}^2 \right) \right] \quad \forall w \in W, p \in P(w), f \in F, t \in T \quad (11)$$

The Conjunctive Normal Form constraints can be then transformed into mixed-integer linear program constraints (12-15) using propositional logic. The value of $Y_{w,p,f,t}^1$ can be determined by $\sum_{\tau \leq t - \tau_C} y_{w,p,f,\tau}^{COMP}$ and the value of $Y_{w,p,f,t}^2$ can be determined by $\sum_{t - \tau_C + 1 \leq \tau \leq t} y_{w,p,f,\tau}^{COMP}$.

$$y_{w,p,f,t}^{SHUTIN} \geq \sum_{t - \tau_C + 1 \leq \tau \leq t} y_{w,p,f,\tau}^{COMP} + \sum_{\tau \leq t - \tau_C} y_{w,p,f,\tau}^{COMP} - 1 \quad \forall w \in W, w' \in W(w), p \in P(w), p' \in P(w'), f \in F, t \in T \quad (12)$$

$$y_{w,p,f,t}^{SHUTIN} \geq \sum_{t - \tau_C + 1 \leq \tau \leq t} y_{w',p',f',\tau}^{COMP} + \sum_{\tau \leq t - \tau_C} y_{w,p,f,\tau}^{COMP} - 1 \quad \forall w \in W, w' \in W(p), p \in P(w), f \in F, f' \in F, t \in T \quad (13)$$

$$y_{w,p,f,t}^{SHUTIN} \leq \sum_{\tau \leq t - \tau_C} y_{w,p,f,\tau}^{COMP} \quad \forall w \in W, f \in F, p \in P(w), t \in T \quad (14)$$

$$y_{w,p,f,t}^{SHUTIN} \leq \sum_{w' \in W(w)} \sum_{p' \in P(w')} \sum_{t - \tau_C + 1 \leq \tau \leq t} y_{w',p',f,\tau}^{COMP} + \sum_{w'' \in W(p)} \sum_{f' \in F} \sum_{t - \tau_C + 1 \leq \tau \leq t} y_{w'',p',f',\tau}^{COMP} \quad \forall w \in W, p \in P(w), f \in F, t \in T \quad (15)$$

Eq. (12) represents that the well should be shut-in if it has been developed and its nearby wells at the same formation are hydraulic fractured. Eq. (13) represents that the well should be shut-in if it has been developed or return-to-pad happens to its connected pad. Eq. (14) enforces that shut-in should only happen after hydraulic fracturing is completed. Eq. (15) enforces that if nor condition one or condition two holds true, shut-in should not happen.

Since the number of Eqs.(12) and (13) is large, we propose another two aggregated formulations as Eqs.(16) and (17), which are equivalent to Eqs.(12) and (13). Though the linear relaxations of Eqs.(12) and (13) is tighter than the linear relaxation of Eqs.(16) and (17), commercial solvers like GUROBI and Cplex can automatically generate minimal cover cuts to further tighten Eqs.(16) and (17).

$$y_{w,f,p,t}^{SHUTIN} \geq \frac{1}{H} \sum_{w' \in W(w)} \sum_{p' \in P(w')} y_{w',p',f,t}^{COMP} + \sum_{\tau \leq t - \tau_C} y_{w,p,f,\tau}^{COMP} - 1 \quad \forall w \in W, p \in P(w), f \in F, t \in T \quad (16)$$

$$y_{w,p,f,t}^{SHUTIN} \geq \frac{1}{H} \sum_{w' \in W(p)} \sum_{f' \in F} \sum_{t - \tau_C + 1 \leq \tau \leq t} y_{w',p',f',\tau}^{COMP} + \sum_{\tau \leq t - \tau_C} y_{w,p,f,\tau}^{COMP} - 1 \quad \forall w \in W, p \in P(w), f \in F, t \in T \quad (17)$$

Rig allocation constraints

In practice, the number of rigs $r \in R$ limits the number of wells that can be developed simultaneously in the shale gas field. During the interval of each drilling batches, rigs should be moved to the next pad and be prepared for the next drilling task. The best allocation of rigs tends to be the minimal movements of rigs since it takes extra money and time to move and relocate rigs. We introduce variable $y_{r,p,t}^{RIG}$ that denotes assignment of each rig r at each period t . Constraint (18) ensures that there is one drilling rig r at pad p as long as any well w is being developed at pad p .

$$\sum_{w \in W(p)} \sum_{f \in F} \sum_{t-\tau_D+1 \leq \tau \leq t} y_{w,p,f,\tau}^{DRILL} \leq \sum_{r \in R} y_{r,p,t}^{RIG} \quad \forall p \in P, t \in T \quad (18)$$

Obviously, a drilling rig r cannot be assigned to more than one well pad at any time.

$$\sum_{p \in P} y_{r,p,t}^{RIG} \leq 1 \quad \forall r \in R, t \in T \quad (19)$$

Since only one well can be developed at each pad at each period, there can be at most one rig at each pad in each period.

$$\sum_{r \in R} y_{r,p,t}^{RIG} \leq 1 \quad \forall p \in P, t \in T \quad (20)$$

Flow balance

Since shale gas production might be interrupted by shut-in, the amount of gas and oil produced by well w can be calculated as Eq. (21), which is represented in Generalized Disjunctive Programming (GDP) form. The production of each well generally follows the predicted production profile. When shut-in occurs, the production at the time period will become zero.

$$\left[\begin{array}{l} \neg \gamma_{w,p,f,t}^{SHUTIN} \\ F_{w,p,f,t}^{GAS} = \sum_{\tau=1}^{t-1} (y_{w,p,f,\tau}^{COMP} \cdot \eta_w \cdot \gamma_{f,t-\tau}^{GAS}) \\ F_{w,p,f,t}^{OIL} = \sum_{\tau=1}^{t-1} (y_{w,p,f,\tau}^{COMP} \cdot \eta_w \cdot \gamma_{f,t-\tau}^{OIL}) \end{array} \right] \vee \left[\begin{array}{l} \gamma_{w,p,f,t}^{SHUTIN} \\ F_{w,p,f,t}^{GAS} = 0 \\ F_{w,p,f,t}^{OIL} = 0 \end{array} \right] \quad \forall w \in W, f \in F, p \in P(w), t \in T \quad (21)$$

where $F_{w,p,f,t}^{GAS}$ and $F_{w,p,f,t}^{OIL}$ are the flow rate of gas and oil produced at well w pad p formation f in time period t , respectively. η_w is the production factor of well w and $\gamma_{f,t-\tau}$ is the well productivity at the age of $t - \tau$ time periods. The big-M reformulation and the convex-hull reformulation of Eq. 21 is presented in Appendix.

The total oil and gas production of pad p can be summed up as Eq. (22)-(23).

$$F_{p,t}^{GAS} = \sum_{w \in W(p)} \sum_{f \in F} F_{w,p,f,t}^{GAS} \quad \forall p \in P, t \in T \quad (22)$$

$$F_{p,t}^{OIL} = \sum_{w \in W(p)} \sum_{f \in F} F_{w,p,f,t}^{OIL} \quad \forall p \in P, t \in T \quad (23)$$

Flow balance should be satisfied at each pad p and gas junction point j in the proposed superstructure. To simplify the index of the flow rate variable, two new sets are introduced here. $m \in M$ is the union of pad set $p \in P$ and junction point set $j \in J$. $n \in N$ is the union of pad set $p \in P$, junction point set $j \in J$ and delivery point q .

For each pad p , the total output flow rate must be equal to the sum of the total input flow rate and the gas produced from the pad as described in Eq.(24). For each gas junction node j , the input flow rate and output flow rate must be equal as described in Eq.(25).

$$\sum_{m \in M_{in}(p)} F_{m,p,t}^{PIPE} + F_{p,t}^{GAS} = \sum_{m \in M_{out}(p)} F_{p,m,t}^{PIPE} \quad \forall p \in P, t \in T \quad (24)$$

$$\sum_{m \in M_{in}(j)} F_{m,j,t}^{PIPE} = \sum_{n \in N_{out}(j)} F_{j,n,t}^{PIPE} \quad \forall j \in J, t \in T \quad (25)$$

where $F_{p,p,t}^{PIPE}$, $F_{j,j,t}^{PIPE}$, $F_{p,j,t}^{PIPE}$ and $F_{j,p,t}^{PIPE}$ are the flowrate in pipelines between pads, between gas junction nodes, from pads to gas junction nodes and from gas junction nodes to pads, respectively.

Pipeline sizing constraints

Generally, the sizes of pipelines is only determined by the flow rates of gas and oil in the gathering network. Pipelines close to the delivery point tend to have larger sizes, while the pipelines far from the delivery point tend to have smaller sizes. However, as we have mentioned above, the production profile of shale gas wells will decline rapidly the first year later after production begins. To avoid poor pipeline utilization, the planning of well development and the sizing of pipelines should be jointly optimized. Since the pipelines are standardized in the oil and gas industry, discrete pipeline diameters $d \in D$ are adopted in this model. Eq. (26) ensures that the flowrate of each pipeline should not exceed its capacity in each period.

$$F_{m,n,t}^{PIPE} \leq \sum_{d \in D} \sum_{\tau \leq t} \delta_d \cdot z_{m,n,d,t}^{PIPE} \quad \forall m \in M, n \in N(m), t \in T \quad (26)$$

where $z_{m,n,d,t}^{PIPE}$ is a binary variable that equals one if the pipeline with diameter d between node m to node n is being installed at time period t .

Since the capacity expansion is not considered in this problem, Eq. (27) states that the diameter of pipelines cannot be changed if selected.

$$\sum_{d \in D} \sum_{t \in T} z_{m,n,d,t}^{PIPE} \leq 1 \quad \forall m \in M, n \in N(m) \quad (27)$$

Objective function

The objective function of the shale gas development problem is to maximize the net present value (NPV). The NPV includes the revenue from selling gas and oil, cost associated with developing wells and production operations, and terminal value of the development project as Eq. (28).

$$\max NPV = \sum_{t \in T} (1 + dr)^{-t} \cdot (REV_t - MOC_t - FPC_t - DVC_t - PCC_t) + \sum_{t \in \hat{T}} (1 + dr)^{-t} \cdot (REV_t - MOC_t) \quad (28)$$

where dr is a discount factor related to the length of each period, REV_t is the revenues from selling natural gas and oil, MOC_t is the maintenance and operation cost, PCC_t is the pad construction cost, FPC_t represents the pipeline installation cost and DVC_t is the drilling and hydraulic fracturing cost, at each time t . The last term in the objective function (28) is the terminal value of the developed well. Since the age limit of shale gas wells is usually much longer than the planning horizon, it makes more sense to include the terminal value into the NPV. An extended horizon \hat{T} is assumed, and only the production revenue and maintenance and the operation cost are accounted for the extended planning periods. To guarantee that the flowrates do not exceed the pipeline capacities in the extended horizon, flow balance constraints are also included in the extended horizon.

The revenues REV_t from selling natural gas and oil within the planning horizon and the extended horizon is defined by Eq.(29).

$$REV_t = (1 - tax) \left(price_{gas} \cdot G \cdot \sum_{p \in P} F_{p,t}^{GAS} + price_{oil} \cdot G \cdot \sum_{p \in P} F_{p,t}^{OIL} \right) \quad \forall t \in T \cup \hat{T} \quad (29)$$

where $price_{gas}$ and $price_{oil}$ are the price of natural gas and oil, G is the length of the time period, tax is the tax that shale gas company needs to pay for selling all gas and oil they produced in this field.

After the development of each well, regular maintenance and operations are required. The maintenance and operation cost is composed of a fixed part representing the basic cost and a variable part that is proportional to the amount of production time. Both the fixed part and the variable part depends on the amount of natural gas and oil produced in each period. Another situation related to maintenance and operation cost is shut-in. When shut-in takes place, the maintenance and operation cost is zero as disjunction (30). The big-M reformulation and the convex-hull reformulation of disjunction (30) is presented in Appendix. In extended periods, no shut-in will happen, so the maintenance and operation cost can be calculated as Eq. (31). The total maintenance and operation cost in each period can be summed as Eq. (32).

$$\left[MOC_{w,p,f,t} = \sum_{\tau=1}^{t-1} y_{w,f,p,\tau}^{COMP} \cdot \eta_w \cdot \left(G \cdot c_{f,t-\tau-\tau_C+1}^{loe-v} + c_{f,t-\tau-\tau_C+1}^{loe-f} \right) \right] \vee \left[\begin{array}{l} \neg Y_{w,p,f,t}^{SHUTIN} \\ MOC_{w,p,f,t} = 0 \end{array} \right] \quad \forall w \in W, f \in F, p \in P(w), t \in T \quad (30)$$

$$MOC_{w,p,f,t} = \sum_{\tau=1}^{t-1} y_{w,f,p,\tau}^{COMP} \cdot \eta_w \cdot \left(G \cdot c_{f,t-\tau-\tau_C+1}^{loe-v} + c_{f,t-\tau-\tau_C+1}^{loe-f} \right) \quad \forall w \in W, f \in F, p \in P(w), t \in \widehat{T} \quad (31)$$

$$MOC_t = \sum_{w \in W} \sum_{p \in P(w)} \sum_{f \in F} MOC_{w,p,f,t} \quad \forall t \in T \cup \widehat{T} \quad (32)$$

The pad construction cost PCC_t includes three parts, surface damage cost, construction cost and return-to-pad cost as Eq. (33). Both surface damage cost and construction cost are proportional to the acreage of the pad. The acreage of each pad is made up of a fixed part, a variable part that is proportional to the number of the wells developed at the pad and another variable part that is proportional to the number of times the return-to-pad happens.

$$PCC_t = (c^{dam} + c^{con}) \cdot \sum_{p \in P} \left[a^f \cdot (y_{p,t}^{rtp-signal} - y_{p,t}^{rtp}) + a^v \cdot \sum_{w \in W(p)} \sum_{f \in F} y_{w,p,f,t}^{DRILL} + a^{rtp} \cdot y_{p,t}^{rtp} \right] + c^{rtp} \cdot \sum_{p \in P} y_{p,t}^{rtp} \quad \forall t \in T \quad (33)$$

where c^{dam} is the unit damage cost per acre, c^{con} is the unit construction cost per acre, a^f is the fixed acreage part of each pad, a^v is the unit variable acreage per well, a^{rtp} is unit variable acreage per return-to-pad.

To calculate the number of occurrences of return-to-pad, two binary variables $y_{p,t}^{rtp}$ and $y_{p,t}^{rtp-signal}$ are introduced. $y_{p,t}^{rtp-signal}$ represents the signal when a drilling batch begins at pad p and $y_{p,t}^{rtp}$ equals one if return-to-pad happens at pad p in time period t . The only difference between $y_{p,t}^{rtp-signal}$ and $y_{p,t}^{rtp}$ is that the first time that $y_{p,t}^{rtp-signal}$ equals one, $y_{p,t}^{rtp}$ equals zero in the planning horizon. Eqs. (34)-(36) together enforce that variable $y_{p,t}^{rtp-signal}$ equals one when a drilling batch takes place at pad p . Eqs. (37)-(39) together enforce that $y_{p,t}^{rtp}$ equals $y_{p,t}^{rtp-signal}$ except the first time $y_{p,t}^{rtp-signal}$ equals one.

$$y_{p,t}^{rtp-signal} \leq \sum_{w \in W(p)} \sum_{f \in F} y_{w,p,f,t}^{DRILL} \quad \forall p \in P, t \in T \quad (34)$$

$$y_{p,t}^{rtp-signal} \leq 1 - \sum_{w \in W(p)} \sum_{f \in F} y_{w,p,f,t-1}^{DRILL} \quad \forall p \in P, t \in T \quad (35)$$

$$y_{p,t}^{rtp-signal} \geq \sum_{w \in W(p)} \sum_{f \in F} y_{w,p,f,t}^{DRILL} - \sum_{w \in W(p)} \sum_{f \in F} y_{w,p,f,t-1}^{DRILL} \quad \forall p \in P, t \in T \quad (36)$$

$$y_{p,t}^{rtp} \leq y_{p,t}^{rtp-signal} \quad \forall p \in P, t \in T \quad (37)$$

$$y_{p,t}^{rtp} \leq \sum_{\tau < t} y_{p,\tau}^{rtp-signal} \quad \forall p \in P, t \in T \quad (38)$$

$$y_{p,t}^{rtp} \geq \frac{1}{H} \sum_{\tau < t} y_{p,\tau}^{rtp-signal} + y_{p,t}^{rtp-signal} - 1 \quad \forall p \in P, t \in T \quad (39)$$

Pipeline construction cost FPC_t in each time period is described by Eq. (40). The cost of the pipelines equals the product of unit price c_d^{pipe} of pipelines and the length $l_{m,n}$ of them.

$$FPC_t = \sum_{m \in M} \sum_{n \in N(m)} \sum_{d \in D} l_{m,n} \cdot c_d^{pipe} \cdot z_{m,n,d,t}^{PIPE} \quad \forall t \in T \quad (40)$$

The development cost DVC_t of each well includes the drilling cost and completion cost. For each drilling batch, there is another fixed start-up cost c^S , including the cost of rig relocation, equipment assembling, equipment disassembling, hydraulic fracturing preparation and etc.

$$DVC_t = \sum_{p \in P} c^S \cdot y_{p,t}^{rtp-signal} + \sum_{w \in W} \sum_{p \in P(w)} \sum_{f \in F} (c_{w,p,f}^D \cdot y_{w,p,f,t}^{DRILL} + c_f^C \cdot y_{w,p,f,t}^{COMP}) \quad \forall t \in T \quad (41)$$

where $c_{w,p,f}^D$ and $c_{w,p,f}^C$ are the drilling cost and hydraulic fracturing cost for each well w at pad p and formation f .

In summary, the proposed model for the shale gas field development problem is formulated as Eq. 42.

$$PO \left\{ \begin{array}{l} \max NPV \\ \text{s.t.} \quad Eqs.(1) - (8), (12) - (41) \end{array} \right\} \quad (42)$$

Bilevel decomposition algorithm

When there are many candidate locations of pads and wells to choose in the shale gas field, the size of the proposed model becomes intractable. The LP(linear program) relaxation of the proposed model is relatively weak, which also makes this model very hard to solve. In this work, we propose a solution pool based bilevel decomposition strategy to solve this problem.

Bilevel decomposition algorithm was first proposed by Iyer and Grossmann [21] to solve the long-range planning problem of process networks. Following this work, Dogan and Grossmann [22] applied the bilevel decomposition algorithm to solve the simultaneous planning and scheduling of single-stage continuous multiproduct plants. Besides the success in solving MILPs, Elsidio et al. [23] combined the bilevel decomposition algorithm with several linearization techniques to solve a MINLP model of simultaneous heat integration and synthesis of steam/organic Rankine cycles problem.

Nowadays, the development of technologies have changed the implementation or even the design of optimization algorithms. A famous example is lazy-benders [24], which uses lazy-constraint callback provided by solvers like Cplex and GUROBI to add benders cuts during the branch and bound process of the master problem. In this work, we combine the solution pool with the bilevel decomposition algorithm. In the bilevel decomposition algorithm, the master problem is a relaxation of the original problem and the subproblem is a fixed original problem. The feasible region of a subproblem is a subset of that of the original problem. The union of the feasible regions of all subproblems should be equivalent to the feasible region of the original problem. Firstly, the algorithm tries to find the subset that most likely includes the optimal solution by solving a relaxed or approximated problem. The subset of the feasible region is then searched by solving the fixed original problem. After each iteration, the explored subset should be cut off from the feasible region. The goal is to combine bilevel decomposition and solution pool is to reduce the number of times the master problem has to be solved. Based on the solution pool, multiple solutions are provided once the master problem is solved, which means several subsets of the feasible region can be explored in each iteration. The reason behind this is that the near-optimal solutions of the master problem can also be helpful for exploring the optimal solution of the full-space model if the master problem is properly defined.

Master problem

Compared with Benders decomposition, Lagrangean decomposition and outer approximation method, bilevel decomposition gives us more freedom of how to define the master problem. The master problem is usually a relaxation or approximation of the original problem. Generally, there are two requirements for a good master problem. 1) The master problem is easier to solve compared with the full-space model. 2) The master problem can provide a valid and tight bound for the full-space model. After some tests, we find that the main complexity of the proposed model lies in shut-in related variables and constraints. Therefore, we relax all the shut-in related constraints and variables in the master problem. Production calculation constraint Eq. (21) is replaced by Eqs. (43)-(44) and MOC_t calculation constraint Eq. (30) is replaced by Eq. (45).

$$F_{w,p,f,t}^{GAS} = \sum_{\tau=1}^{t-1} (y_{w,p,f,\tau}^{COMP} \cdot \eta_w \cdot \gamma_{f,t-\tau}^{GAS}) \quad \forall w \in W, f \in F, p \in P(w), t \in T \quad (43)$$

$$F_{w,p,f,t}^{OIL} = \sum_{\tau=1}^{t-1} (y_{w,p,f,\tau}^{COMP} \cdot \eta_w \cdot \gamma_{f,t-\tau}^{OIL}) \quad \forall w \in W, f \in F, p \in P(w), t \in T \quad (44)$$

$$MOC_{w,p,f,t} = \sum_{\tau}^{t-1} y_{w,p,\tau}^{COMP} \cdot \eta_w \cdot \left(G \cdot c_{f,t-\tau-\tau_C+1}^{Ioe-v} + c_{f,t-\tau-\tau_C+1}^{Ioe-f} \right) \quad \forall w \in W, f \in F, p \in P(w), t \in T \quad (45)$$

The test result also shows that pipeline installation cost only accounts for a small part of the total cost. To simplify the master problem, the flow balance constraint and pipeline sizing constraint are replaced by Eq. (46) and the net present value is calculated as Eq. (47).

$$\sum_{w \in W} \sum_{p \in P(w)} \sum_{f \in F} F_{w,p,f,t}^{GAS} \leq \delta_{max} \quad (46)$$

$$\max NPV = \sum_{t \in \bar{T}} (1 + dr)^{-t} \cdot (REV_t - MOC_t - DVC_t - PCC_t) + \sum_{t \in \bar{T}} (1 + dr)^{-t} \cdot (REV_t - MOC_t) \quad (47)$$

The master problem is finally defined by Eq.(48). There are two properties of the master problem. First, the master problem P_M is a relaxation of the original problem and can provide an upper bound for it. If the master problem cannot be solved to optimality in a limited time, we can use the upper bound of the master problem as an upper bound of the original problem. Second, the feasible solution of the master problem is a part of a feasible solution of the full-space model. This is because shut-in will not only interrupt production and lead to the decline of gas flow and oil flow. The only constraint that limits the gas flow is the pipeline capacity constraint. If the gas flow without shut-in satisfies the pipeline capacity constraint, the gas flow with shut-in should also satisfy the pipeline capacity constraint.

$$P_M \left\{ \begin{array}{l} \max NPV \\ s.t. \text{ Eqs. (1) - (8), (18) - (20), (22) - (23), (29), (31) - (39), (41), (43) - (46)} \end{array} \right\} \quad (48)$$

| Subproblem

As we have mentioned above, bilevel decomposition is a master-problem-guided search algorithm. The scale of the subproblem determines the region that can be searched for each subproblem. There is a tradeoff between the scale of the subproblem and the efficiency to solve it. If the scale of the subproblem is large and cannot be solved efficiently, each iteration may take a long time. If the scale of the subproblem is small, it may take many iterations for the algorithm to converge. Therefore, we propose two different subproblems for the proposed model.

| subproblem A

Among all the variables in the original problem, $y_{w,p,f,t}^{DRILL}$ and $y_{w,p,f,t}^{COMP}$ can be regarded as key variables. Once $y_{w,p,f,t}^{DRILL}$ and $y_{w,p,f,t}^{COMP}$ are fixed, $y_{w,p,f,t}^{SHUTIN}$ can be determined according to Eq. (9), $y_{p,t}^{rtpsignal}$ and $y_{p,t}^{rtp}$ can be determined according to Eq. (36)-(39). Flowrate $F_{w,p,f,t}^{GAS}$ and $F_{w,p,f,t}^{OIL}$ can also be determined by Eq. (21). Other variables, like $y_{r,p,t}^{RIG}$, $y_{n,n',t}^{PIPE}$ and $z_{n,n',d,t}^{PIPE}$ can be limited for the most part. Therefore, we fix variable $y_{w,p,f,t}^{DRILL}$ and $y_{w,p,f,t}^{COMP}$ in the subproblem A according to the solution of the master problem. Let $\bar{y}_{w,p,f,t}^{DRILL}$ and $\bar{y}_{w,p,f,t}^{COMP}$ be the solution of master problem. The subproblem is defined as the original problem subject to Eqs.(49) - (50).

$$y_{w,p,f,t}^{DRILL} = \bar{y}_{w,p,f,t}^{DRILL} \quad \forall w \in W, p \in P(w), f \in F, t \in T \quad (49)$$

$$y_{w,p,f,t}^{COMP} = \bar{y}_{w,p,f,t}^{COMP} \quad \forall w \in W, p \in P(w), f \in F, t \in T \quad (50)$$

The subproblem is defined by Eq. (48). Since shut-in will result in a reduction of gas and oil production, we keep $z_{n,n',d,t}^{PIPE}$ unfixed and the diameter of the pipelines can be reoptimized when solving the subproblem.

$$P_{SA} \left\{ \begin{array}{l} \max NPV \\ \text{s.t.} \quad \text{Eqs. (1) - (8), (12) - (41), (49) - (50)} \end{array} \right\} \quad (51)$$

After solving the subproblem A, we can add an integer cut to the master problem to exclude the previously obtained feasible solution. The integer cut is defined as Eq. (52).

$$\sum_{(w,p,f,t) \in Z_1^D} y_{w,p,f,t}^{DRILL} - \sum_{(w,p,f,t) \in Z_0^D} y_{w,p,f,t}^{DRILL} + \sum_{(w,p,f,t) \in Z_1^C} y_{w,p,f,t}^{COMP} - \sum_{(w,p,f,t) \in Z_0^C} y_{w,p,f,t}^{COMP} \leq |Z_1^D| + |Z_1^C| - 1 \quad (52)$$

where $Z_0^D = \{(w, p, f, t) | \bar{y}_{w,p,f,t}^{DRILL} = 0\}$, $Z_1^D = \{(w, p, f, t) | \bar{y}_{w,p,f,t}^{DRILL} = 1\}$, $Z_0^C = \{(w, p, f, t) | \bar{y}_{w,p,f,t}^{COMP} = 0\}$ and $Z_1^C = \{(w, p, f, t) | \bar{y}_{w,p,f,t}^{COMP} = 1\}$.

| subproblem B

Since the shut-in related constraints and variables are all relaxed in the master problem and shut-in is determined by the scheduling of completion operation, another way to define the subproblem is only fixing the network of the shale gas field instead of the detailed scheduling decisions. This will give the subproblem more freedom to find a better solution but makes the subproblem harder to solve. The network can be fixed according to the solution of the master problem through Eqs (53).

$$\sum_{t \in T} y_{w,p,f,t}^{DRILL} \leq \sum_{t \in T} \bar{y}_{w,p,f,t}^{DRILL} \quad \forall w \in W, p \in P(w), f \in F \quad (53)$$

$$\sum_{t \in T} y_{w,p,f,t}^{COMP} \leq \sum_{t \in T} \bar{y}_{w,p,f,t}^{COMP} \quad \forall w \in W, p \in P(w), f \in F \quad (54)$$

Due to the existence of Eq. (8), either of Eqs. (53) and (54) is enough to fix the network. Here we choose Eq. (8) as an example. The subproblem is defined as Eq. (55)

$$P_{SB} \left\{ \begin{array}{l} \max NPV \\ \text{s.t.} \quad (1) - (8), (12) - (41), (53) - (54) \end{array} \right\} \quad (55)$$

After solving the subproblem, both the integer cut and the subset cut should be added to exclude the explored

solutions from the master problem. The integer cut is defined as Eq.(56) and the subset cut is defined as Eqs. (57).

$$\sum_{(w,p,t) \in Z_1} \sum_{t \in T} y_{w,p,f,t}^{DRILL} - \sum_{(w,p,f) \in Z_0} \sum_{t \in T} y_{w,p,f,t}^{DRILL} \leq |Z_1| - 1 \quad (56)$$

$$\sum_{(w,p,f) \in Z_0} \sum_{t \in T} y_{w,p,f,t}^{DRILL} + \sum_{t \in T} y_{w',p',f',t'}^{DRILL} \geq 1 \quad \forall (w',p',f') \in Z_1 \quad (57)$$

where $Z_0 = \{(w,p,f) \mid \sum_{t \in T} \bar{y}_{w,p,f,t}^{DRILL} = 0\}$ and $Z_1 = \{(w,p,f) \mid \sum_{t \in T} \bar{y}_{w,p,f,t}^{DRILL} = 1\}$.

| Solution pool based bilevel decomposition

The flowchart of the proposed algorithm is presented in Figure 3. First, the master problem is solved and the solution pool is obtained. The master problem can provide an upper bound to the original problem. Based on the solution pool, we first rank and filter the solutions in the solution pool according to the objective value and bound of each solution. Next, several subproblems are created according to the solutions in the solution pool. Since the subproblem is a fixed original problem, it can provide a lower bound to the original problem. If the lower bound lies within a tolerance of the upper bound, the algorithm will terminate. Otherwise, the current solution will be removed from the solution pool. Integers and logic cuts are added to the master problem. The inner iteration will not end until the solution pool is empty. A comprehensive iteration process of the proposed solution pool based bilevel decomposition algorithm is shown in Figure 4.

There are two possible reasons we choose the solution pool instead of lazy constraint callback [25] for the bilevel decomposition algorithm. One possible reason why lazy constraints callback may not be inappropriate for bilevel decomposition is that the subset chosen by the master problem is usually near-optimal in each iteration. However, the lazy constraints callback is activated whenever a feasible integer solution is found. The solutions obtained in the early stage of the branch and bound tree are often far away from the optimal solution of the full space problem. It would probably waste time solving the subproblems based on the early-stage solutions of the master problem. Another possible reason is that in both benders decomposition algorithm and outer approximation algorithm, Benders cut and OA cuts will not cut off integer solution of the original problem and a reformulation can be obtained with all the cuts. However, in the bilevel decomposition algorithm, integer cut or subset cut will be added to the master problem.

Case Study

To illustrate the application of the MILP model and the efficiency of the proposed algorithm, five examples of different scales are considered in this section. In these five examples, an untapped shale gas field with two formations is considered. The only difference among these five examples is the number of candidate well locations and candidate pad locations. The data of these five examples are in Table 1. We consider a 2-year planning horizon and an extended 3-year horizon to calculate the terminal value of this field. The 2-year planning horizon is discretized into 48 planning periods with an equal length of half a month. The drilling process takes one time period $\tau_C = 1$ and the completion process takes half of the time period $n_1^C = 2$. In one time period, at most six completion operations can be implemented simultaneously $n_2^C = 6$. The discount rate is 10% per year and the tax rate is 9%. The price of gas is 2.72 \$/MCF and

the price of oil is 69.1\$/BBL. The production factor of all 16 sections in the 80 wells & 60 pads example is presented in Table 4. The production factor of all 16 sections in the 80 wells & 60 pads example is presented in Table 4. The relative gas capacity and unit cost of each pipeline is shown in Table 2. The acreage data of pad construction is presented in Table 3. All these data derive from a real-world shale gas development project. For confidentiality reasons, we cannot disclose the exact cost data of pad construction, drilling and completion, nor the exact production profile of each candidate well. The cost of drilling a 3D well is about 20% more expensive than 2D well. The cost of drilling in formation 2 is about 2% more expensive than formation 1 and the cost of completion in formation 2 is 10% less expensive than formation 1. The relative daily oil and gas gross production of the wells in both formations are shown in Figure 5.

Our implementation is based on the Pyomo [26] and the runs are conducted on an Intel® Xeon® CPU 2.67 GHz processor with 128 GB of available RAM. The mixed-integer linear programs were solved using the IBM ILOG CPLEX Optimizer 12.10.0.0, which we restricted to a single CPU thread for a fair comparison among runs.

Comparison of Model Tractability

In section 4, we present two different formulations for both the operation sequence constraint, i.e., (3) v.s. (4) and the shut-in logic constraint, i.e., (12) and (13) v.s. (16) and (17). The disjunctions (21) and (30) can also be reformulated in two ways, big-M reformulation and convex-hull reformulation. Therefore, there are 8 different combinations of the formulation. We first solve all these formulations of the five cases directly using Cplex. The statistics of each formulation and a summary of the tests are presented in Table 5. For confidentiality reasons, we cannot disclose the exact value of the NPV and the upper bound in Table 5. Only the relative optimality gap is presented.

In table 5, the number of variables is only affected by the reformulation method of the shut-in disjunctions, while the number of constraints is affected by all three constraints. Compared with big-m reformulation, convex-hull reformulation introduces new variables. For instance, the 5 wells & 5 pads example has 68,491 continuous variables when big-M reformulation is applied and this number becomes 6,169 continuous variables when convex-hull reformulation is applied. The time-disaggregated formulation and convex-hull reformulations introduce more constraints. In the 5 wells & 5 pads example, the combination has the largest number of constraints, i.e., 131,456.

Although the convex-hull reformulation introduces new variables and constraints, the LP relaxation of convex-hull reformulation has been proved to be tighter than the big M reformulation. From the results in Table 5, we can see that there is no formulation that dominates all the others in all five examples. For the 80 wells & 60 pads example, no feasible solution is found within 10 hours for all eight formulations. For the rest of the examples, the four formulations with convex-hull reformulated disjunctions outperform the other four formulations with big-M reformulated disjunction on average. We can conclude that compared with big-M reformulation, the convex-hull reformulation of disjunctions (21) and (30) will make the problem much easier to solve. In the 30 wells & 20 pads example, the best formulation is the one with time-aggregated operational sequence constraint, big-M based logic constraints and convex-hull reformulated disjunctions, which finds the best solution with a 66.18% optimality gap. For the 20 wells & 10 pads example and the 5 wells & 5 pads example, the formulation of time-aggregated operational sequence constraint, convex-hull based logic constraints and convex-hull reformulated disjunctions outperforms other formulations. In the 10 wells & 5 pads example, the best formulation is the one with time-disaggregated operational sequence constraint, convex-hull based logic constraints and convex-hull reformulated disjunctions. Since we focus more on the tractability of larger examples, we choose the formulation of time-aggregated operational sequence constraint, big-M based logic constraints and Convex-hull reformulated disjunctions as the base model. Further tests of bilevel decomposition are based on this formulation.

| The effect of bilevel decomposition algorithm

With the baseline in table 5, the solution pool based bilevel decomposition algorithm is applied to solve the problem. The comparison of the scale of the full-space model and the master problem is shown in table 6. Taking the 80 wells & 60 pads case as an example, the number of binary variables, continuous variables and constraints of the master problem has been reduced by 40.6%, 99.0%, 97.2%, which makes the master problem much easier to solve.

The results of the bilevel decomposition algorithm and the solution pool based bilevel decomposition algorithm is shown in table 7 and table 8, respectively. The objective improvement column refers to the gap between the best objective values found by bilevel decomposition method and direct solving. In the 5 wells & 5 pads example, the bilevel decomposition algorithm both with and without solution pool (subproblem B) can find the optimal solution in the first iteration. However, the bilevel decomposition algorithm both with and without solution pool (subproblem A) can only find near optimal solution. Since the explored region in subproblem A is more limited, it takes the bilevel decomposition algorithm without solution pool (subproblem A) a few more iterations for the algorithm to find a good solution. However, since the solution pool enables the algorithm to explore more regions in one iteration, a near optimal solution can be found by bilevel decomposition algorithm with solution pool (subproblem A) within fewer iterations. One drawback of bilevel decomposition algorithm (subproblem A) is that subproblem A will become increasingly harder to solve with the accumulation of integer cuts. In other larger examples, the bilevel decomposition algorithm (subproblem A) outperforms the bilevel decomposition algorithm (subproblem B). For instance, for the 80 wells & 60 pads, the bilevel decomposition algorithm (subproblem A) can obtain the best solution with a 17.59% optimality gap and the bilevel decomposition algorithm (subproblem B) can only obtain the solution with a 40.64% gap. Overall, solution pool is more helpful to bilevel decomposition algorithm with subproblem A. This is because that solution pool is used to reduce the times of solving master problems. Compared with both master problem and subproblem B, subproblem A is much easier to solve. The majority of the time in bilevel decomposition(subproblem A) is consumed in solving the master problem. Therefore, the solution pool can obviously accelerate the convergence of bilevel decomposition algorithm (subproblem A).

Since the master problem is a relaxation of the original problem, we use the upper bound of the master problem as the final bound when the master problem cannot be solved to optimality. Therefore, the calculated gap is always overestimated and consists of two components. The first part is the gap of the master problem if it is not solved to optimality within the time limit. The second part is the reduction of the NPV when shut-in constraints and pipeline cost are included. Generally, the second part accounts for the majority of the final gap. For example, when we use solution pool based bilevel decomposition(subproblem A) to solve the 80 wells & 60 pads example, the gap of the master problem and the decline of NPV respectively account for 49.7% and 50.3% of the final gap.

| Result analysis

In all the five examples, we choose the 5 wells & 5 pads example, the 30 wells & 20 pads example and the 80 wells & 60 pads example for further analysis. The solutions analyzed here are from Table 7, which are obtained using bilevel decomposition algorithm.

The shale gas network of the optimal solution of the 5 wells & 5 pads case is presented in Figure 6. All wells are developed as 2D well, which coincides with the fact that developing 2D wells takes fewer resources. As we have mentioned above, for multiple-well pad, drilling batch saves time and money for the development and will not result in shut-in. It happens in Figure 8a, such as pad 1, pad2 and pad 5. For instance, well 1 at formation 1 and well 1 at formation 2 will be drilled sequentially in time period 1 and time period 2. Then, both wells are completed together

in time period 3. The size of the pipelines is all eight inches. The relative oil and gas production profile of each pad is presented in Figure 7. The peak of the total gas production reaches 66.7% of the pipeline capacity.

To figure out the impact of shut-in, we compare the optimal solution of the original problem P_O and the master problem P_M . Both optimal solutions have the same shale gas network as Figure 6. Figure 8a is the detailed operation scheduling of the original problem P_O . Figure 8b is the detailed operation scheduling of a fixed original problem, whose operation variables are fixed according to the optimal solution master problem P_M . The development of the shale gas field completes in four periods and drilling batch happens four times in both solutions. The number of wells developed in each period is the same in both solutions, one well in the second period, six wells in the third period and three wells in the fourth period. Therefore, the difference between the two solutions is only the sequence of development operations. Through proper scheduling of development operations, the number of shut-in is reduced from 8 to 4. On average, the whole production is brought forward by 0.4 periods. The proper operations sequence increases the NPV by 1.7%.

Figure 9 shows the shale gas network of the optimal solution for the 30 wells & 20 pads example. All the candidate wells and pads are developed in the planning horizon and all the developed wells are 2D well. Since formation 2 is more productive, wells in formation 2 will be first developed. In most of the pads, two to four wells are developed. The number of wells that can be developed from one pad is indirectly constrained by the shut-in conditions. If a larger multiple-well pad is planned and the wells are developed in a large drilling batch, this will lead to the delay of production for the early drilled wells. If these wells are developed at intervals, shut-in will happen several times according to the constraint (9), which will lead to production interruption. The size of the pipelines follows the tendency of gas production accumulation along with the pipeline network. For example, the size of the pipeline between pad 1 and pad 10 is 8 inches, while the size of the pipeline between junction node 4 and delivery node is set to the biggest size of 12 inches. The Gantt chart of the optimal development solution is shown in Figure 10. After 30 planning periods, all the wells will be developed. One consequence of developing all candidate wells is that shut-in happens 140 times totally, which corresponds to the red blocks in the Gantt chart.

The relative production profile of gas and oil in the shale gas field is shown in Figure 11 and Figure 12. In the first 15 periods, the production level of gas and oil continues increasing and reaches the peak. After that, the production profile becomes flat and fluctuates frequently. The fluctuations result from the shut-in of working wells since the production suddenly becomes zero for the shut-in wells. The flattening of the production profile is due to the pipeline capacity. The production profile in Figure 11 equals the flow rate in the pipeline between junction node 4 and the delivery node. The pipeline between the junction node and the delivery node is pipeline 12". After the rapid development in the first 15 periods, the production profile approaches the pipeline capacity, which coincides to the development slowing down after 15 periods in Figure 10. It is the pipeline capacity that limits the speed of the development. Only when the production of developed wells declines, there will be free space for new wells. For this reason, return-to-pad happens 40 times during the planning horizon. For example, well 3 in formations 2 is developed from pad 3 during time period 11 and 12. Since the total production profile approaches the pipeline capacity limit, it waits until time period 27 to develop well 3 in formation 1. During the fluctuating periods, shut-in also serves a method to prevent the gas flow exceeding the pipeline capacity. If shut-in is removed from the development plan, the gas flow in several periods will exceed the pipeline capacity. When all the wells are developed, the gas production profile will decline continuously in the remaining periods.

Figure 13 shows the shale gas network of the optimal solution of the 80 wells & 60 pads example. Compared with the optimal solution of the 30 wells & 20 pads example, only half of the candidate wells are developed in the planning horizon. Since the formation 2 is more productive, most of the developed wells are in formation 2. Similar to the network in Figure 9, all the developed wells are 2D well and most of the pads connect to 2 to 4 wells in Figure

13. The closer the pipeline is to the delivery node, the bigger the size of the pipeline is.

Figure 14 represents the detailed scheduling of the development. In general, the wells in Formation1 are first developed and the wells in formation2 will be developed later. This is because that formation1 has a higher production profile according to Figure 5. In figure 14, we also find that the development slows down after 12 periods. Therefore, we plot the total relative production profile of gas and oil in figure 15 and figure 16 . After the rapid growth in the first 12 periods, the flow rate approaches the capacity of the 12-inch pipeline. The flat and fluctuating phase will last until the end of the planning horizon. Return-to-pad takes place 23 times during the planning horizon and most of it happens during the flat and fluctuating phase. After all the developments in two years, the total production profile declines continuously in the extended time periods.

The pie chart of the revenues and costs is presented in Figure 17. Overall, the revenue is about 2 times of the total cost. Oil and gas respectively account for 89.5% and 10.5% of the total revenue. The well development cost account for the largest proportion ,about 77.9%, of the total cost. The maintenance and operation cost is about 17.9%, and the pad construction cost is about 3.9% of the total cost. The pipeline installation cost accounts for the smallest part 0.3% of the total cost.

Generally, the profit of shale gas development are greatly affected by the oil and gas prices. A sensitivity analysis is carried out for the 80 wells & 60 pads example to determine the minimum oil and gas prices for a cost-effective development. The result is presented in Figure 18. Ten different oil prices and ten different gas prices are selected according to the historical market data. To keep consistency in the different tests, the same drilling decisions and hydraulic fracturing decisions as in Figure 13 is applied. The NPV when gas price equals 2.72 \$/MCF and oil price equals 69.1 \$/BBL is selected as the baseline and the baseline prices correspond to the red point in Figure 18. The relative NPV is presented at each block of the heat map. According to Figure 18, the NPV is more sensitive to the fluctuation of oil price. It's also not hard to find that when the oil price becomes 33 \$/BBL and the gas price price becomes 2.4 \$/MCF, the development is break-even. If the oil and gas prices are below this, it's not profitable to develop the shale gas field.

In summary, for the 20 wells & 30 pads example and 60 wells & 80 pads example, the limitation of the problem is the capacity of the pipeline. The optimal solution first develops wells as fast as possible to approach the capacity limit. Then the development slows down and new wells are developed to maintain this level when the production profile declines.

Conclusion

In this work, we have proposed a discrete-time MILP model to address the multi-formation shale gas field development problem. Motivated by real-world cases, the proposed superstructure allows each candidate well to have several alternative pads. Therefore, the proposed model focuses on the drilling operation and completion operations of each well and the connection between wells and pads. Based on the sequence of operations, pad drilling batch is also considered in this model. It is more consistent with the practice where several wells are first sequentially drilled and then hydraulically fractured together, saving them time and money to move and relocate rigs. Furthermore, to guarantee the safety of the whole development, two shut-in conditions are modeled using Generalized Disjunctive Programming. For each working well, the production will stop while other nearby wells at the same formation are being completed and when return-to-pad happens.

Since the model becomes intractable for commercial solvers, a bilevel decomposition algorithm is proposed and the solution pool is also applied to enhance the algorithm's performance. Two different subproblems are defined. The results of five different examples show that the proposed algorithm can effectively solve the shale gas field development problem. A much better solution can be found within limited time compared with directly solving with commercial solvers. The results on realistic instances show how the optimal development strategy increases the net present value by limiting the size of the multi-well pads and avoiding shut-ins. When the gathering system capacity limits the development speed, the optimal development strategy makes good use of return-to-pad operations to maximize the utilization of the pipeline network.

Future work will concentrate on the uncertainties in shale gas field development, including the oil and gas price, the demands from downstream plants, the production profile of each well and the breakdown of development facilities.

Nomenclature

| Sets

$w \in W$ = candidate wells

$w \in W(p)$ = candidate wells for pad p

$w' \in W(w)$ = candidate wells near well w

$p \in P$ = candidate pads

$p \in P(w)$ = candidate pads for well w

$f \in F$ = formations

$j \in J$ = gas junction points

q = gas delivery point

$n \in N$ = node set including pads, gas junction points and gas delivery point

$m \in M$ = node set including pads and gas junction points

$m' \in M_{in}(m)$ = node n' that directly connected to node m and the flow direction is from m' to m

$m' \in M_{out}(m)$ = node n' that directly connected to node m and the flow direction is from m to m'

$n' \in N_{out}(m)$ = node n' that directly connected to node n and the flow direction is from m to n

$t, \tau \in T$ = time periods

$d \in D$ = pipeline diameters

d_{max} = max pipeline diameters

$r \in R = \text{rigs}$

Parameters

η_w = production factor of well w

H = a very big number

$\gamma_{w,t-\tau}^{GAS}$ = gas productivity at well w of age $t - \tau$

$\gamma_{w,t-\tau}^{OIL}$ = oil productivity at well w of age $t - \tau$

δ_d = gas capacity of pipeline with diameter d

δ_{max} = maximal gas capacity of all alternative pipelines

n_1^C = upper limit for the number of wells that can be hydraulically fractured at each pad simultaneously

n_2^C = upper limit for the total number of wells that can be hydraulically fractured in each time period

dr = discount rate

tax = tax for selling gas and oil

G = the length of each time period

$c_{f,t-\tau}^{loev}$ = the variable cost of loe in formation f of age $t - \tau$

$c_{f,t-\tau}^{loef}$ = the fix cost of loe in formation f of age $t - \tau$

$price_{gas}$ = the price of gas

$price_{oil}$ = the price of oil

c^{dam} = cost of surface damage

c^{con} = cost of construction

c^{rtp} = cost of return to pad

c^S = fixed start-up cost

a^f = fixed acreage

a^v = variable acreage

a^{rtp} = return to pad acreage

c_d^{pipe} = cost of pipeline in diameter d

$l_{m,n}$ = the distance between node m and node n

$c_{w,p,f}^D$ = cost of drilling at well w , pad p , formation f

$c_{w,p,f}^C$ = cost of completion at well w , pad p , formation f

τ_D = the number of periods for drilling operation

τ_C = the number of periods for completion operation

Variables

Binary variables

$y_{w,p,f,t}^{DRILL}$ = if wells w in formation f start being drilled at pad p during period t (action)

$y_{w,p,f,t}^{COMP}$ = if wells w in formation f start being completed at pad p during period t (action)

$y_{w,p,f,t}^{SHUTIN}$ = if wells w in formation f at pad p should be shut-in during period t

$y_{r,p,t}^{RIG}$ = if drilling rig r is on pad p in time period t

$z_{n,n',d,t}^{PIPE}$ = if pipeline between node n and node n' with diameter d is being installed in time period t

$y_{p,t}^{rtp-signal}$ = if a drilling batch begins in time period t , which is a return to pad signal

$y_{p,t}^{rtp}$ = if return to pad happens at pad p in time period t

Boolean variables

$Y_{w,p,f,t}^{SHUTIN}$ = True if well w in formation f connected to pad p shut-in in time period t

$Y_{w,p,f,t}^1$ = True if well w in formation f connected to pad p has been developed in time period t

$Y_{w,p,f,t}^2$ = True if well w in formation f connected to pad p is being completed in time period t

Continuous variables

$F_{p,t}^{GAS}$ = the flowrate of gas produced at pad p in time period t

$F_{w,p,f,t}^{GAS}$ = the flowrate of gas produced at well w pad p formation f in time period t

$F_{p,t}^{OIL}$ = the flowrate of oil produced at pad p in time period t

$F_{w,p,f,t}^{OIL}$ = the flowrate of oil produced at well w pad p formation f in time period t

$F_{n,n',t}^{PIPE}$ = the flowrate of gas from node n to node n' in time period t

REV_t = Revenues from natural gas and oil sales in time period t

MOC_t = Production and maintenance cost in time period t

PCC_t = pad construction cost in time period t

FPC_t = Flow pipeline construction cost in time period t

DVC_t = Development cost (drilling, completion) in time period t

NPV = Net present value of the shale gas development project

acknowledgements

The authors gratefully acknowledge financial support from SK innovation, Center for Advanced Process Decision-making, Carnegie Mellon University. Zedong Peng gratefully acknowledges the financial support from the China Scholarship Council (CSC) (No. 201906320320) and the Science Fund for Creative Research Groups of NSFC (No. 61621002).

references

- [1] Administration USEI, Annual Energy Outlook 2020 with projections to 2050;. Available at <https://www.eia.gov/outlooks/aeo/pdf/AEO2020%20Full%20Report.pdf> (2020/07/28).
- [2] Allen RC, Allaire D, El-Halwagi MM. Capacity planning for modular and transportable infrastructure for shale gas production and processing. *Industrial & Engineering Chemistry Research* 2018;58(15):5887–5897.
- [3] Cafaro DC, Grossmann IE. Strategic planning, design, and development of the shale gas supply chain network. *AIChE Journal* 2014;60(6):2122–2142.
- [4] Drouven MG, Grossmann IE. Multi-period planning, design, and strategic models for long-term, quality-sensitive shale gas development. *AIChE Journal* 2016;62(7):2296–2323.
- [5] Ondeck A, Drouven M, Blandino N, Grossmann IE. Multi-operational planning of shale gas pad development. *Computers & Chemical Engineering* 2019;126:83–101.
- [6] Gao J, You F. Shale gas supply chain design and operations toward better economic and life cycle environmental performance: MINLP model and global optimization algorithm. *ACS Sustainable Chemistry & Engineering* 2015;3(7):1282–1291.

-
- [7] Gao J, You F. Economic and environmental life cycle optimization of noncooperative supply chains and product systems: modeling framework, mixed-integer bilevel fractional programming algorithm, and shale gas application. *ACS Sustainable Chemistry & Engineering* 2017;5(4):3362–3381.
- [8] Gao J, You F. Integrated hybrid life cycle assessment and optimization of shale gas. *ACS Sustainable Chemistry & Engineering* 2018;6(2):1803–1824.
- [9] Chebeir J, Asala H, Taleghani AD, Romagnoli JA. The Application of Reservoir Simulation to the Optimization of Shale Gas Supply Chain Design and Its Water Management Structure. In: *Computer Aided Chemical Engineering*, vol. 40 Elsevier; 2017.p. 1435–1440.
- [10] Yang L, Grossmann IE, Mauter MS, Dilmore RM. Investment optimization model for freshwater acquisition and wastewater handling in shale gas production. *AIChE Journal* 2015;61(6):1770–1782.
- [11] Drouven MG, Grossmann IE. Optimization models for impaired water management in active shale gas development areas. *Journal of Petroleum Science and Engineering* 2017;156:983–995.
- [12] Guerra OJ, Calderón AJ, Papageorgiou LG, Siirola JJ, Reklaitis GV. An optimization framework for the integration of water management and shale gas supply chain design. *Computers & Chemical Engineering* 2016;92:230–255.
- [13] Cafaro DC, Drouven MG, Grossmann IE. Optimization models for planning shale gas well refracture treatments. *AIChE Journal* 2016;62(12):4297–4307.
- [14] Cafaro DC, Drouven MG, Grossmann IE. Continuous-time formulations for the optimal planning of multiple refracture treatments in a shale gas well. *AIChE Journal* 2018;64(5):1511–1516.
- [15] Asala HI, Chebeir JA, Manee V, Gupta I, Dahi-Taleghani A, Romagnoli JA, et al. An integrated machine-learning approach to shale-gas supply-chain optimization and refrac candidate identification. *SPE Reservoir Evaluation & Engineering* 2019;.
- [16] Knudsen BR, Foss B. Shut-in based production optimization of shale-gas systems. *Computers & Chemical Engineering* 2013;58:54–67.
- [17] Zeng Z, Cremaschi S. Artificial lift infrastructure planning for shale gas producing horizontal wells. *Proceedings of the FOCAPO/CPC, Tuscan, AZ, USA 2017*;p. 8–12.
- [18] Li X, Armagan E, Tomasgard A, Barton PI. Stochastic pooling problem for natural gas production network design and operation under uncertainty. *AIChE Journal* 2011;57(8):2120–2135.
- [19] Wang H, Lappas NH, Gounaris CE. Multi-mode Resource Constrained Project Scheduling with Alternative Prerequisites: New Models and Computational Studies. *Industrial & Engineering Chemistry Research* 2019;58(39):18253–18266.
- [20] Trespalacios F, Grossmann IE. Review of mixed-integer nonlinear and generalized disjunctive programming methods. *Chemie Ingenieur Technik* 2014;86(7):991–1012.
- [21] Iyer RR, Grossmann IE. A bilevel decomposition algorithm for long-range planning of process networks. *Industrial & Engineering Chemistry Research* 1998;37(2):474–481.
- [22] Dogan ME, Grossmann IE. A decomposition method for the simultaneous planning and scheduling of single-stage continuous multiproduct plants. *Industrial & engineering chemistry research* 2006;45(1):299–315.
- [23] Elsidio C, Martelli E, Grossmann IE. A bilevel decomposition method for the simultaneous heat integration and synthesis of steam/organic Rankine cycles. *Computers & Chemical Engineering* 2019;128:228–245.
- [24] Lin S, Lim GJ, Bard JF. Benders decomposition and an IP-based heuristic for selecting IMRT treatment beam angles. *European Journal of Operational Research* 2016;251(3):715–726.

-
- [25] Corporation I, IBM ILOG CPLEX Optimization Studio CPLEX User's Manual;. Available at https://www.ibm.com/support/knowledgecenter/SSSA5P_12.8.0/ilog.odms.studio.help/pdf/usrcplex.pdf (2020/08/26).
- [26] Hart WE, Laird CD, Watson JP, Woodruff DL, Hackebeil GA, Nicholson BL, et al. Pyomo-optimization modeling in python, vol. 67. Springer; 2017.

List of figure captions

Figure 1: US Energy production and the dry natural gas production

Figure 2: The proposed shale gas field superstructure

Figure 3: Flow chart of the solution pool based bilevel decomposition algorithm

Figure 4: Iteration process of the solution pool based bilevel decomposition algorithm

Figure 5: Relative oil and gas production profile and relative variable MOC part of the two formations

Figure 6: Shale gas network of 5 wells & 5 pads example

Figure 7: Relative gas and oil production profile of the 5 wells & 5 pads example

Figure 8: Comparison of the solution of the model with and without shut-in

Figure 9: Shale gas network of 30 wells & 20 pads example

Figure 10: Gantt chart of the 30 wells & 20 pads shale gas field development

Figure 11: Relative gas production profile of the 30 wells & 20 pads shale gas field

Figure 12: Relative oil production profile of the 30 wells & 20 pads shale gas field

Figure 13: Shale gas network of the 80 wells & 60 pads example

Figure 14: Gantt chart of the 80 wells & 60 pads shale gas field development

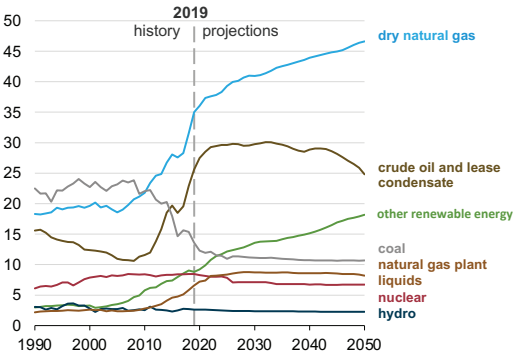
Figure 15: Relative gas production profile of the 80 wells & 60 pads shale gas field

Figure 16: Relative oil production profile of the 80 wells & 60 pads shale gas field

Figure 17: The revenue and costs of the 80 wells & 60 pads example

Figure 18: Sensitivity analysis on the oil and gas prices

Energy production
quadrillion British thermal units



Dry natural gas production by type
trillion cubic feet

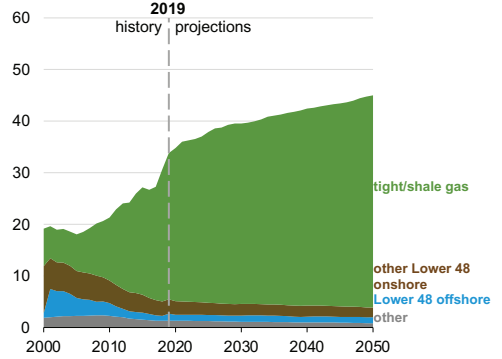


FIGURE 1 US Energy production and the dry natural gas production[1]

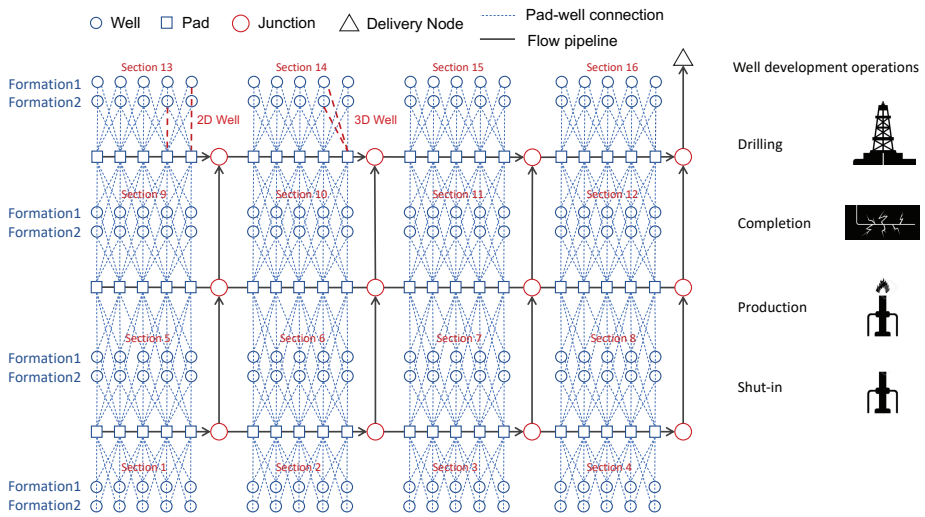


FIGURE 2 The proposed shale gas field superstructure

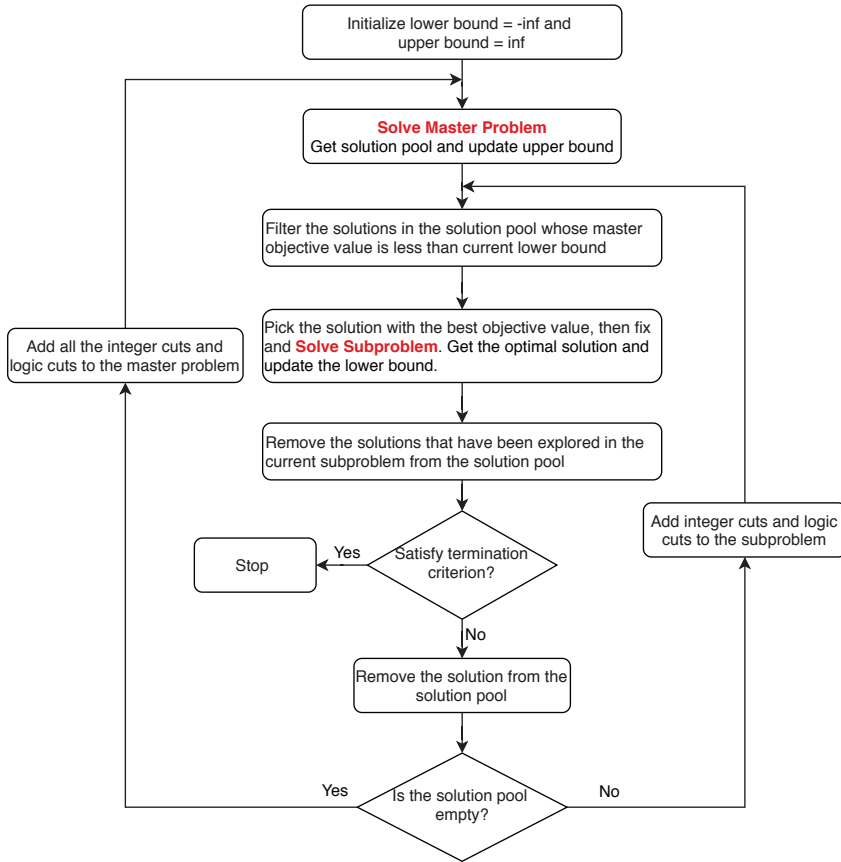


FIGURE 3 Flow chart of the solution pool based bilevel decomposition algorithm

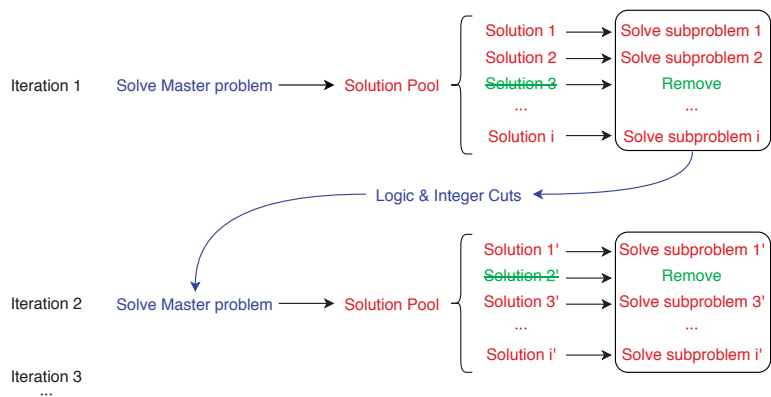


FIGURE 4 Iteration process of the solution pool based bilevel decomposition algorithm

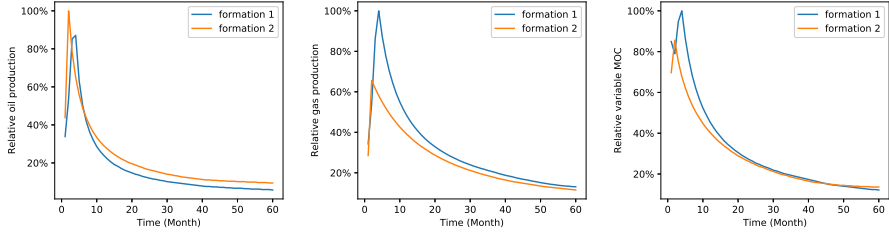


FIGURE 5 Relative oil and gas production profile and relative variable MOC part of the two formations

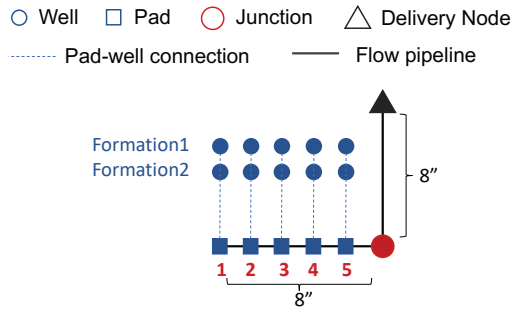
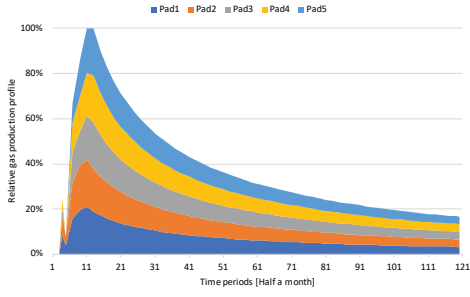
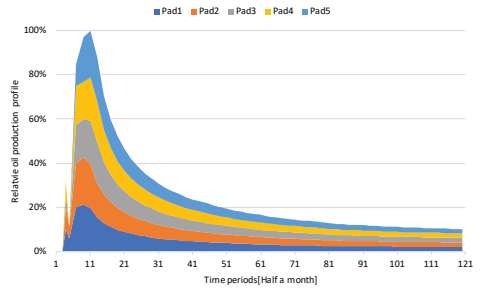


FIGURE 6 Shale gas network of 5 wells & 5 pads example

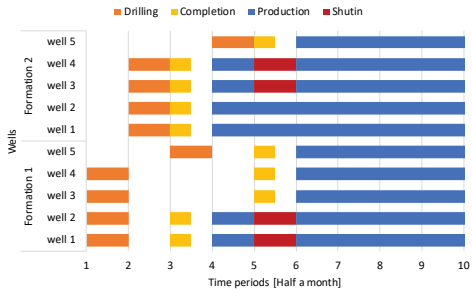


(a) Relative gas production

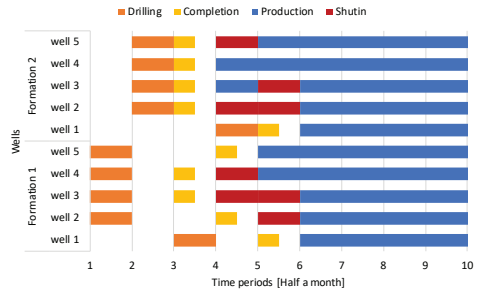


(b) Relative oil production

FIGURE 7 Relative gas and oil production profile of the 5 wells & 5 pads example



(a) With shut-in



(b) Without shut-in

FIGURE 8 Comparison of the solution of the model with and without shut-in

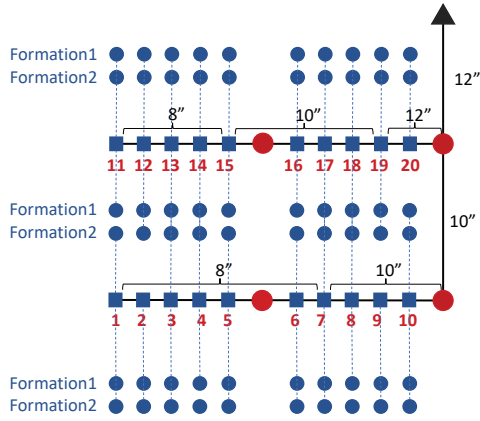


FIGURE 9 Shale gas network of 30 wells & 20 pads example

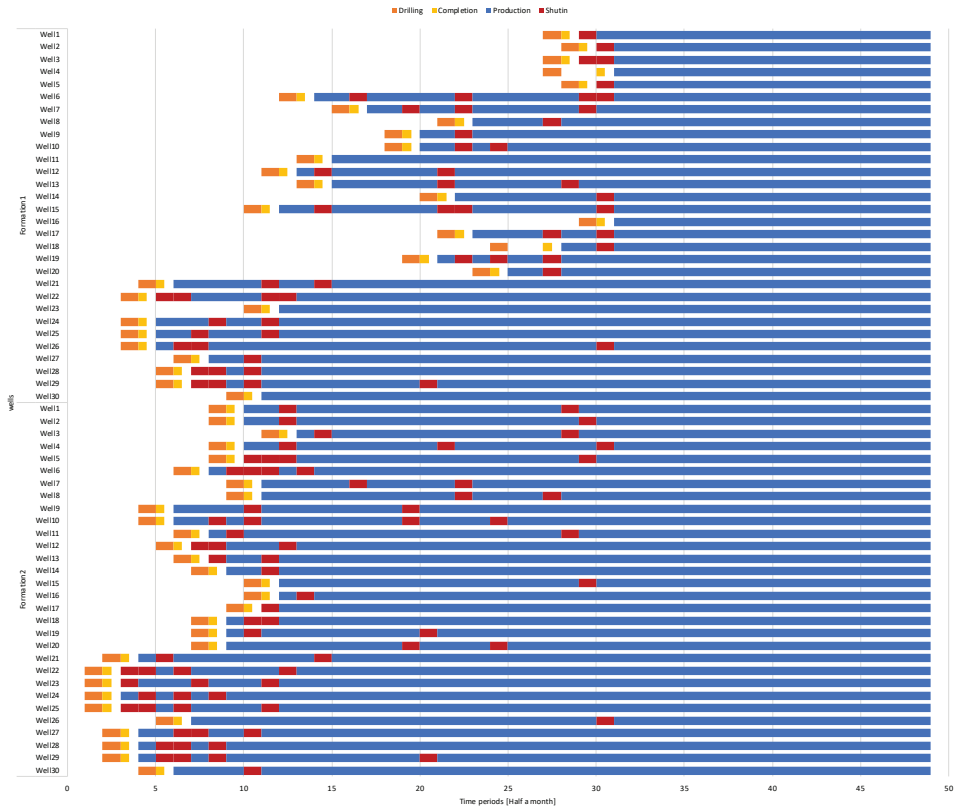


FIGURE 10 Gantt chart of the 30 wells & 20 pads shale gas field development

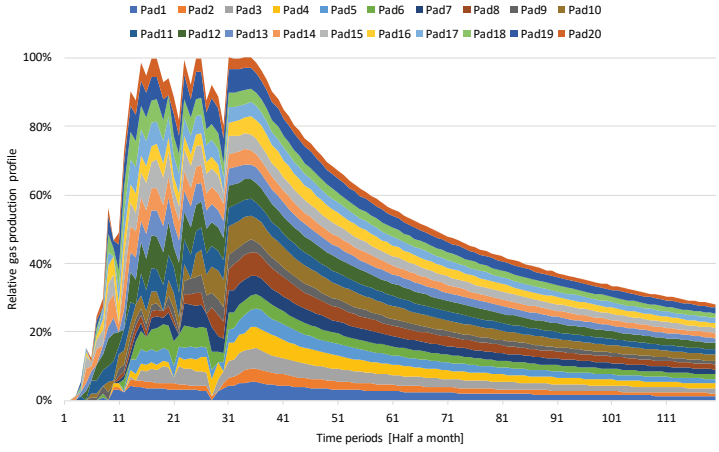


FIGURE 11 Relative gas production profile of the 30 wells & 20 pads shale gas field

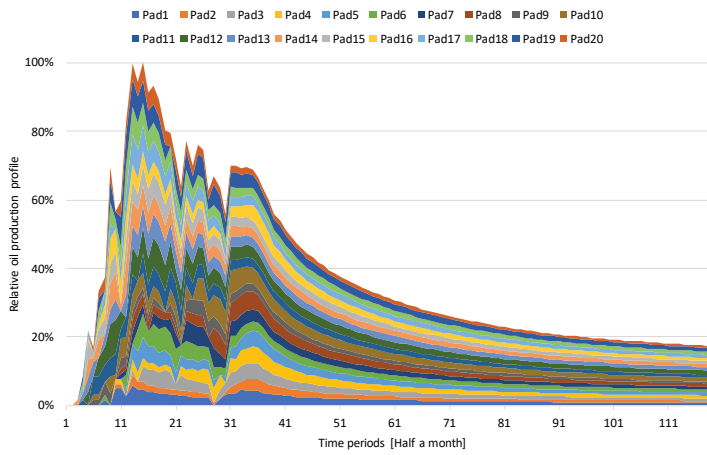


FIGURE 12 Relative oil production profile of the 30 wells & 20 pads shale gas field

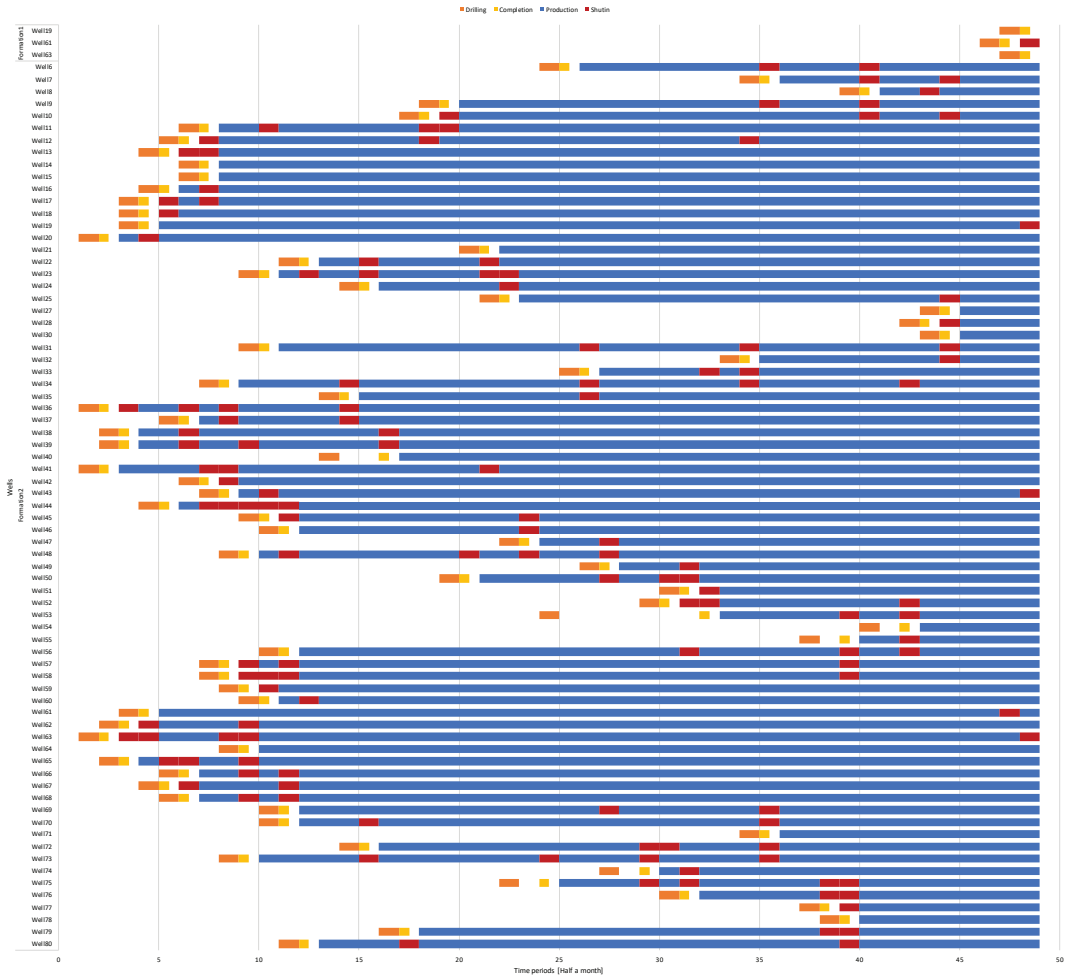


FIGURE 14 Gantt chart of the 80 wells & 60 pads shale gas field development

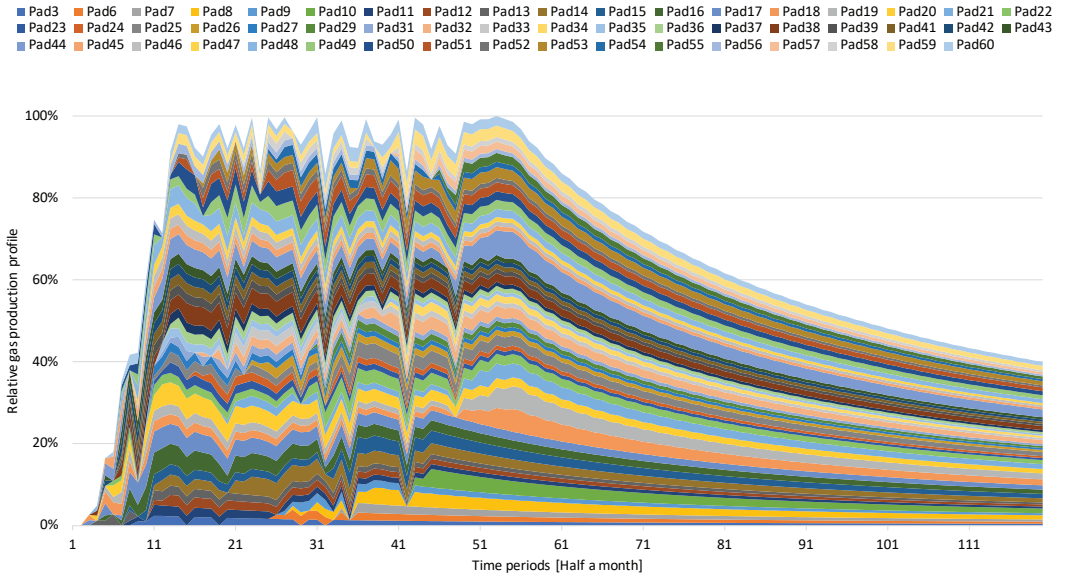


FIGURE 15 Relative gas production profile of the 80 wells & 60 pads shale gas field

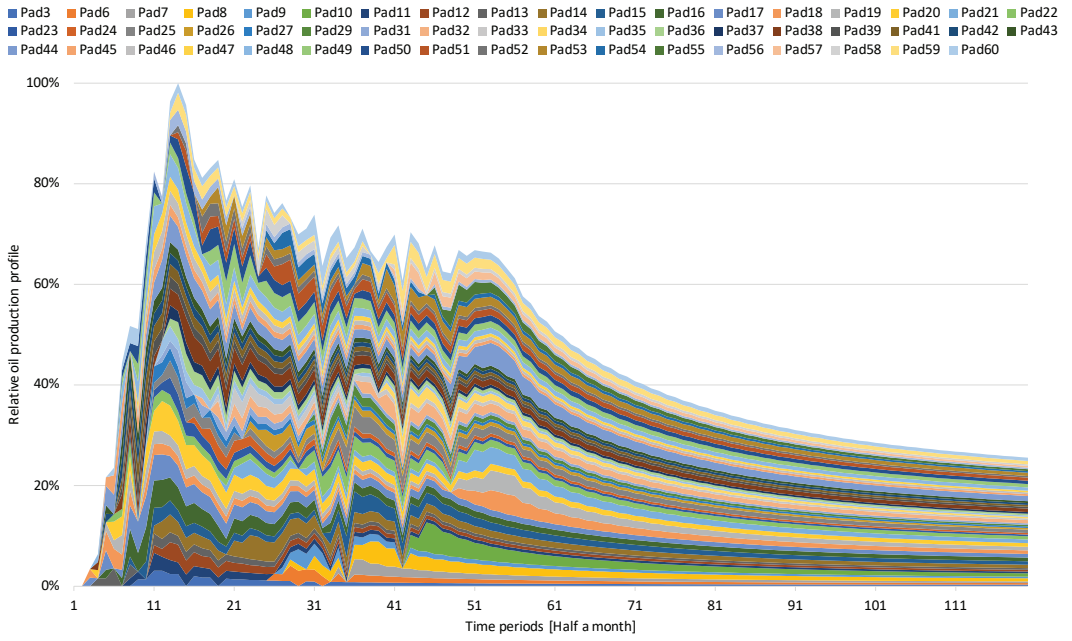
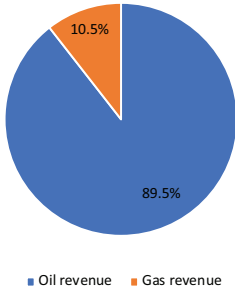
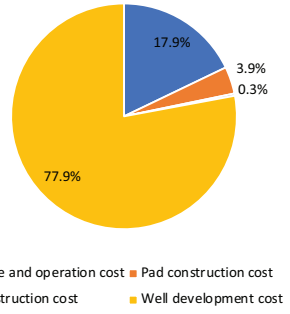


FIGURE 16 Relative oil production profile of the 80 wells & 60 pads shale gas field



(a) Revenues



(b) Costs

FIGURE 17 The revenue and costs of the 80 wells & 60 pads example



FIGURE 18 Sensitivity analysis on the oil and gas prices

TABLE 1 The number of candidate well locations and candidate pad locations of the five examples

Examples	# of candidate well locations	# of candidate pad locations
1	5	5
2	10	5
3	20	10
4	30	20
5	80	60

TABLE 2 The relative gas capacity and unit cost of pipelines

Pipeline ID	Relative gas capacity	Relative unit cost
8"	33.9%	44.8%
10"	61.5%	71.2%
12"	100.0%	100.0%

TABLE 3 Acreage data of pad construction

Category	Acreage
Fixed Acreage (acres/pad)	1.8
Variable Acreage (acres/well)	0.2
Return-to-Pad (rtp) Acreage (acres/rtp)	0.5

TABLE 4 Production factor of each section in 80 wells & 60 pads example

Section	Section 1	Section 2	Section 3	Section 4	Section 5	Section 6	Section 7	Section 8
Production Factor	0.8	0.95	1.1	1.2	0.95	0.85	1	1.15
Section	Section 9	Section 10	Section 11	Section 12	Section 13	Section 14	Section 15	Section 16
Production Factor	1.05	0.85	0.9	1.05	1.2	1.1	1	0.95

TABLE 5 Computational results of different formulation directly solved by Cplex

Examples	Operation sequence constraint	shut-in logic constraint	Disjunction	# of all variables	# of binary variables	# of continuous variables	# of constraints	Gap	CPU time(s)
5 wells & 5 pads	Aggregated	Big M	Big M	13,465	7,296	6,169	28,312	39.21%	36,000
5 wells & 5 pads	Aggregated	Convex hull	Big M	13,465	7,296	6,169	42,328	4.68%	36,000
5 wells & 5 pads	Disaggregated	Big M	Big M	13,465	7,296	6,169	29,534	26.71%	36,000
5 wells & 5 pads	Disaggregated	Convex hull	Big M	13,465	7,296	6,169	43,550	10.94%	36,000
5 wells & 5 pads	Aggregated	Big M	Convex hull	75,787	7,296	68,491	116,218	3.75%	36,000
5 wells & 5 pads	Aggregated	Convex hull	Convex hull	75,787	7,296	68,491	130,234	2.47%	36,000
5 wells & 5 pads	Disaggregated	Big M	Convex hull	75,787	7,296	68,491	117,440	5.30%	36,000
5 wells & 5 pads	Disaggregated	Convex hull	Convex hull	75,787	7,296	68,491	131,456	3.73%	36,000
10 wells & 5 pads	Aggregated	Big M	Big M	22,201	12,288	9,913	50,838	43.18%	36,000
10 wells & 5 pads	Aggregated	Convex hull	Big M	22,201	12,288	9,913	92,310	30.70%	36,000
10 wells & 5 pads	Disaggregated	Big M	Big M	22,201	12,288	9,913	53,282	45.03%	36,000
10 wells & 5 pads	Disaggregated	Convex hull	Big M	22,201	12,288	9,913	94,754	32.31%	36,000
10 wells & 5 pads	Aggregated	Big M	Convex hull	146,845	12,288	134,557	226,650	14.79%	36,000
10 wells & 5 pads	Aggregated	Convex hull	Convex hull	146,845	12,288	134,557	268,122	15.34%	36,000
10 wells & 5 pads	Disaggregated	Big M	Convex hull	146,845	12,288	134,557	229,094	18.09%	36,000
10 wells & 5 pads	Disaggregated	Convex hull	Convex hull	146,845	12,288	134,557	270,566	9.76%	36,000
20 wells & 10 pads	Aggregated	Big M	Big M	44,017	24,576	19,441	101,051	-	36,000
20 wells & 10 pads	Aggregated	Convex hull	Big M	44,017	24,576	19,441	190,139	-	36,000
20 wells & 10 pads	Disaggregated	Big M	Big M	44,017	24,576	19,441	105,939	190.58%	36,000
20 wells & 10 pads	Disaggregated	Convex hull	Big M	44,017	24,576	19,441	195,027	-	36,000
20 wells & 10 pads	Aggregated	Big M	Convex hull	293,305	24,576	268,729	452,675	24.34%	36,000
20 wells & 10 pads	Aggregated	Convex hull	Convex hull	293,305	24,576	268,729	541,763	18.80%	36,000
20 wells & 10 pads	Disaggregated	Big M	Convex hull	293,305	24,576	268,729	457,563	33.08%	36,000
20 wells & 10 pads	Disaggregated	Convex hull	Convex hull	293,305	24,576	268,729	546,651	148.92%	36,000
30 wells & 20 pads	Aggregated	Big M	Big M	87,649	49,152	38,497	201,457	817.71%	36,000
30 wells & 20 pads	Aggregated	Convex hull	Big M	87,649	49,152	38,497	424,945	-	36,000
30 wells & 20 pads	Disaggregated	Big M	Big M	87,649	49,152	38,497	211,233	664.52%	36,000
30 wells & 20 pads	Disaggregated	Convex hull	Big M	87,649	49,152	38,497	434,721	-	36,000
30 wells & 20 pads	Aggregated	Big M	Convex hull	586,225	49,152	537,073	904,705	66.18%	36,000
30 wells & 20 pads	Aggregated	Convex hull	Convex hull	586,225	49,152	537,073	1,128,193	70.68%	36,000
30 wells & 20 pads	Disaggregated	Big M	Convex hull	586,225	49,152	537,073	914,481	207.15%	36,000
30 wells & 20 pads	Disaggregated	Convex hull	Convex hull	586,225	49,152	537,073	1,137,969	117.41%	36,000
80 wells & 60 pads	Aggregated	Big M	Big M	262,177	147,456	114,721	603,101	-	36,000
80 wells & 60 pads	Aggregated	Convex hull	Big M	262,177	147,456	114,721	1,349,597	-	36,000
80 wells & 60 pads	Disaggregated	Big M	Big M	262,177	147,456	114,721	632,429	-	36,000
80 wells & 60 pads	Disaggregated	Convex hull	Big M	262,177	147,456	114,721	1,378,925	-	36,000
80 wells & 60 pads	Aggregated	Big M	Convex hull	1,757,905	147,456	1,610,449	2,712,845	-	36,000
80 wells & 60 pads	Aggregated	Convex hull	Convex hull	1,757,905	147,456	1,610,449	3,459,341	-	36,000
80 wells & 60 pads	Disaggregated	Big M	Convex hull	1,757,905	147,456	1,610,449	2,742,173	-	36,000
80 wells & 60 pads	Disaggregated	Convex hull	Convex hull	1,757,905	147,456	1,610,449	3,488,669	-	36,000

TABLE 6 Comparison of the scale of full-space model and master problem

Examples	Full space model			Master problem		
	# of binary variables	# of continuous variables	# of constraints	# of binary variables	# of continuous variables	# of constraints
5 wells & 5 pads	7,296	68,491	116,218	4,800	1,705	5,770
10 wells & 5 pads	12,288	134,557	226,650	7,296	1,705	7,080
20 wells & 10 pads	24,576	268,729	452,675	14,592	3,025	13,415
30 wells & 20 pads	49,152	537,073	904,705	29,184	5,665	26,065
80 wells & 60 pads	147,456	1,610,449	2,712,845	87,552	16,225	76,685

TABLE 7 Computational results of bilevel decomposition with subproblemA

Examples	Bilevel decomposition without solution pool (SubproblemA)				Bilevel decomposition with solution pool (SubproblemA)			
	Optimality gap	Objective improvement	CUP time(s)	Iterations	Optimality gap	Objective improvement	CUP time(s)	Iterations
5 wells & 5 pads	4.33%	-0.58%	3344	68	3.19%	0.51%	1994	42
10 wells & 5 pads	7.03%	6.82%	17028	34	7.01%	6.82%	800	1
20 wells & 10 pads	15.90%	7.36%	25207	7	15.22%	8.05%	3602	1
30 wells & 20 pads	20.67%	36.40%	36002	1	20.42%	36.50%	32400	1
80 wells & 60 pads	17.59%	-	32406	1	18.47%	-	32408	1

TABLE 8 Computational results of bilevel decomposition with subproblemB

Examples	Bilevel decomposition without solution pool (SubproblemB)				Bilevel decomposition with solution pool (SubproblemB)			
	Optimality gap	Objective improvement	CUP time(s)	Iterations	Optimality gap	Objective improvement	CUP time(s)	Iterations
5 wells & 5 pads	2.62%	1.07%	10820	1	2.62%	1.07%	5286	1
10 wells & 5 pads	9.06%	5.27%	32600	1	6.85%	6.91%	36000	1
20 wells & 10 pads	19.26%	4.46%	36000	1	17.50%	5.95%	36000	1
30 wells & 20 pads	24.95%	31.83%	36000	1	37.26%	19.79%	36000	1
80 wells & 60 pads	40.64%	-	36000	1	40.70%	-	36000	1